

Annual South American forest loss estimates based on passive microwave remote sensing (1990-2010)

M. J. E. van Marle¹, G. R. van der Werf¹, R. A. M. de Jeu^{1,2} and Y. Y. Liu³

[1]{Faculty of Earth and Life Sciences, Vrije Universiteit Amsterdam, Amsterdam, the Netherlands}

[2]{now at Transmissivity B.V., Space Technology Centre, Noordwijk, the Netherlands}

[3]{ARC Centre of Excellence for Climate System Science & Climate Change Research Centre, University of New South Wales, Sydney, Australia}

Correspondence to: M. J. E. van Marle (m.j.e.van.marle@vu.nl)

Abstract

Consistent forest loss estimates are important to understand the role of forest loss and deforestation in the global carbon cycle, for biodiversity studies, and to estimate the mitigation potential of reducing deforestation. To date, most studies have relied on optical satellite data and new efforts have greatly improved our quantitative knowledge on forest dynamics. However, most of these studies yield results for only a relatively short time period or are limited to certain countries. We have quantified large-scale forest loss over a 21-year period (1990-2010) in the tropical biomes of South America using remotely sensed vegetation optical depth (VOD). This passive microwave satellite-based indicator of vegetation water content and vegetation density has a much coarser spatial resolution than optical data but its temporal resolution is higher and VOD is not impacted by aerosols and cloud cover. We used the merged VOD product of the Advanced Microwave Scanning Radiometer (AMSR-E) and Special Sensor Microwave Imager (SSM/I) observations, and developed a change detection algorithm to quantify spatial and temporal variations in forest loss dynamics. Our results compared reasonably well with the newly developed Landsat-based Global Forest Change (GFC) maps, available for the 2001 onwards period ($r^2=0.90$ when comparing annual country-level estimates). This allowed us to convert our identified changes in VOD to forest loss area and compute these from 1990 onwards. We also compared these calibrated results to

1 PRODES ($r^2=0.60$ when comparing annual state-level estimates). We found that South
2 American forest exhibited substantial interannual variability without a clear trend during the
3 1990s, but increased from 2000 until 2004. After 2004, forest loss decreased again, except for
4 two smaller peaks in 2007 and 2010. For a large part, these trends were driven by changes in
5 Brazil, which was responsible for 56% of the total South American forest loss area over our
6 study period according to our results. One of the key findings of our study is that while forest
7 loss decreased in Brazil after 2005, increases in other countries partly offset this trend
8 suggesting that South American forest loss as a whole decreased much less than that in Brazil.

9

10 **1 Introduction**

11 There are large uncertainties in the spatial and temporal patterns of forest loss and associated
12 fluxes of carbon in the tropical ecosystems (Grainger, 2008; Hansen et al., 2010; Malhi, 2010;
13 Pan et al., 2011). Forest loss can be either natural, for example due to wind-throw or natural
14 fires, or anthropogenic, usually labelled deforestation. Deforestation carbon emissions are a
15 significant but declining fraction of total anthropogenic CO₂ emissions (van der Werf et al.,
16 2009). In Amazonia, tropical deforestation was the main source of carbon emissions (Morton
17 et al., 2008), at least during their 2003 to 2007 study period. More than half of the total forest
18 carbon is stored in tropical intact forests, where more than 50% is stored in living biomass,
19 about a third in the soil and the remaining carbon is stored in dead wood and litter (Pan et al.,
20 2011). In South America, deforestation is mainly caused by expansion of agriculture and area
21 used for cattle ranging (FAO, 2006; Fearnside, 2005; Geist and Lambin, 2002), and the
22 continent is responsible for almost half of the tropical deforestation emissions (Harris et al.,
23 2012; Pan et al., 2011). Over the last 30 years soybean production has expanded rapidly in
24 Amazonia, partly driven by improved yield-increasing and labour-saving technologies (Grau
25 et al., 2005; Naylor et al., 2005).

26 Historically, widely used datasets for forest area changes and timber harvesting in the 80s and
27 90s are the forest resource assessments (FRAs), as reported by countries to the United Nations
28 Food and Agriculture Organization (UN FAO) (FAO, 2006), but which are known to suffer
29 from issues regarding consistency (Grainger, 2008). Satellite observations overcome some of
30 the issues found in earlier FAO datasets, because they systematically monitor in space and
31 time. Over the last three decades several satellite-based deforestation datasets have been
32 developed. Landsat satellite imagery is the longest operative option for monitoring vegetation.

1 From 1972 through January 1999 the Landsat Multispectral Scanner (MSS) provided
2 continuous data on relatively high spatial resolution of 90 meter. From 1982 onwards the
3 Landsat (Enhanced) Thematic Mapper ((E)TM) provides vegetation cover on an even higher
4 spatial resolution of 30 meter, with a 16-day revisit time. However, the effective temporal
5 resolution is much lower because of cloud cover issues, which often persists not only in the
6 wet season but also during the dry season between June and November in the Amazon basin
7 south of the equator (Costa and Foley, 1998). Therefore, these observations are mostly used in
8 annual or multi-year analyses, but there is a need for alternative non-optical data techniques to
9 provide time-series on a monthly or higher temporal resolution (Asner, 2001). Other widely
10 used satellite datasets for vegetation are the Normalized Difference Vegetation Index (NDVI),
11 often derived from the Advanced Very High Resolution Radiometer (AVHRR). NDVI is
12 sensitive to canopy greenness (Anyamba and Tucker, 2005; Tucker et al., 2005; Zhu et al.,
13 2013). This dataset has a higher temporal, but coarser spatial resolution than Landsat, and is
14 also sensitive to aerosols and cloud cover. Other vegetation datasets that can capture
15 vegetation dynamics are for example the observations based on long-wavelength radar
16 backscatter (Joshi et al., 2015), where deforestation, forest degradation and the follow-up
17 vegetation cover could be captured, and those based on observations from the SeaWinds Ku-
18 band scatterometer (Frolking et al., 2012), which have shown to capture gross forest loss in
19 the tropics. Also lidar data can be used to estimate forest biomass, and can thus capture
20 vegetation dynamics (Mitchard et al., 2012). Data availability for radar and lidar datasets is
21 usually from 1998 onwards.

22 Over the past years, the number of datasets quantifying vegetation dynamics, carbon stocks
23 and other relevant vegetation quantities on both global and regional scale has thus increased
24 substantially, often using Landsat and AVHRR data but also other data sources including the
25 Moderate-resolution Imaging Spectroradiometer (MODIS, launched in 1999 on board of
26 Terra and in 2002 on Aqua), Medium Resolution Imaging Spectrometer (MERIS, 2002-2012)
27 and Satellite Pour l'Observation de la Terre Vegetation Program (SPOT VGT, from 1986
28 onboard different satellites) (Acharid et al., 2014; Baccini et al., 2012; Broich et al., 2011;
29 Ernst et al., 2013; Eva et al., 2012; Frolking et al., 2012; Jones et al., 2011; de Jong et al.,
30 2013; Kim et al., 2015; Koh et al., 2011; Mayaux et al., 1998; Morton et al., 2005; Potapov et
31 al., 2012; Saatchi et al., 2011; Verbesselt et al., 2012; Verhegghen et al., 2012; Wasige et al.,
32 2012).

1 One of the regions most closely monitored is the Brazilian Legal Amazon, where the
2 Brazilian National Institute for Space Research (INPE) developed the Program for
3 Deforestation Assessment in the Brazilian Legal Amazon with Satellite Imagery (PRODES).
4 PRODES estimates annual deforestation since 1988 based on a multi-data approach mostly
5 based on Landsat data but also the China-Brazil Earth Resource Satellite (CBERS-2B) and
6 UK-DCM2 from the Disaster Monitoring Constellation International Imaging (DMCii)
7 (Shimabukuro et al., 1998). Other efforts include the recently published global maps of global
8 forest gain and loss for the 2001-2012 period also using Landsat data (Hansen et al., 2013).

9 In addition to the previously mentioned datasets mostly based on visible and infrared
10 wavelengths, passive microwave observations can also be used to characterize vegetation
11 dynamics. Vegetation optical depth (VOD) is a vegetation attenuation parameter in the
12 microwave domain. This parameter was first described by Kirdiashev et al. (1979) in a zero-
13 order radiative transfer model for vegetation canopies. VOD is primarily sensitive to the
14 vegetation water content and also captures information about vegetation structure (Jackson
15 and Schmugge, 1991; Kerr and Njoku, 1990; Kirdiashev et al., 1979).

16 The longer wavelengths of passive microwave enables sensitivity of VOD not only to the
17 leafy part, but also to woody parts of vegetation (Andela et al., 2013). Therefore VOD yields
18 information about both the photosynthetic and non-photosynthetic parts of aboveground
19 vegetation, based on the water content (Jones et al., 2011; Shi et al., 2008). VOD is shown to
20 be highly correlated with aboveground biomass (Liu et al., 2011a; Owe et al., 2001) and thus
21 yields information about the net forest loss; the balance between decreases in forest loss due
22 to deforestation and degradation and increases in forest extend due to regrowth or thickening.
23 Furthermore, the advantage of low frequency (<20 GHz) microwave remote sensing is that
24 aerosols and clouds have a negligible effect on the observations, so even areas with regular
25 cloud cover are observed frequently, which makes it suitable to use for global vegetation
26 monitoring at daily time steps.

27 Comparing AVHRR NDVI and passive microwave based VOD datasets with a record longer
28 than 20 years, Liu et al. (2011) showed that both datasets had similar seasonal cycles. VOD
29 however, also showed interannual variations in regions with water stress, which corresponds
30 for a large part to variations in precipitation. VOD was more sensitive to changes in woody
31 vegetation compared to NDVI, whereas NDVI was more sensitive to herbaceous changes
32 (Andela et al. 2013). This is the result of NDVI being more sensitive to canopy greenness

1 (Myneni et al., 1995) and VOD being more sensitive to water content, relatively speaking.
2 Thus, when forest is converted to large-scale cropland, the canopy greenness does not
3 necessarily drop, whereas the total water content of the aboveground biomass decreases (Liu
4 et al., 2011a).

5 The main disadvantage of these low-frequency passive observations is that a large footprint is
6 needed to yield an observable signal, making this dataset most suitable for large regional and
7 continental-scale studies. These retrievals therefore have a relatively coarse resolution,
8 compared to observations in the visible and near infrared parts of the spectrum. Furthermore
9 the presence of open water regions affects the signal. This, in combination with the large
10 footprint of the gridded product, may lead to underestimation of VOD when grid cells are
11 close to large open waters (Jones et al., 2011). VOD is retrieved from several satellite sensors.
12 The observations retrieved from the Advanced Microwave Scanning Radiometer (AMSR-E)
13 and Special Sensor Microwave Imager (SSM/I) have been merged to one dataset with a
14 spatial resolution of 0.25° , based on Cumulative Distribution Function (CDF) matching. This
15 merged VOD dataset has been used to study vegetation dynamics in different ecosystems on
16 both global and regional scales (Andela et al., 2013; Liu et al., 2012, 2013, 2015; Poulter et
17 al., 2014; Zhou et al., 2014). Guan et al. (2012) compared QuickScat Ku-band backscatter
18 coefficients (dB) with VOD and NDVI and noted that the three datasets are comparable, but
19 that dB shows abnormal high values when more bare soil is present in the pixel.

20 This paper aims to estimate large-scale forest loss in South America. We show how the
21 merged VOD product can be used to estimate forest loss for South America on a country-
22 level scale, but we also point towards limitations of our approach and the dataset. The main
23 novelty of our approach is the relatively long (1988-2011) time series based on a consistent
24 data stream. We detail how we translated the VOD signal to forest loss area by calibrating our
25 results to the Global Forest Change maps of Hansen et al. (2013), which are subsequently
26 compared to the Landsat-derived PRODES dataset. We provide a country-level analysis of
27 the newly derived maps, and zoom in on Brazil to present a state-level analysis of forest loss
28 over the 1990-2010 period. This time period is somewhat shorter than the time span of the
29 VOD dataset due to the requirements of the change detection algorithm we developed.

30

1 **2 Datasets**

2 In this section we describe the datasets we used in our analysis. First, we give more
3 information on the VOD dataset that is used for our estimation of forest loss (Sect 2.1),
4 followed by describing the two datasets we used for comparison: the Global Forest Change
5 (GFC, Sect. 2.2), which besides being used for comparing the spatio-temporal variability is
6 also used to translate our results to area estimates, and the PRODES dataset (Sect. 2.3).

7 **2.1 Vegetation Optical Depth (VOD)**

8 Forest loss estimates in this article are based on VOD, which is derived from passive
9 microwave remote sensing. Passive microwave remote sensing differs from active microwave
10 remote sensing (radar) in the sense that radar transmits a long-wavelength microwave signal
11 through the atmosphere and then records the amount of energy backscattered, whereas passive
12 systems record electromagnetic energy that was reflected or emitted from the surface of the
13 Earth. VOD was first introduced by Kirdiashev et al. (1979), and then modified to be used in
14 the well-known omega-tau model (Mo et al., 1982). Kirdiashev et al. (1979) already described
15 the relationship between VOD and vegetation water content. This relationship was further
16 simplified by Jackson and Schmugge (1991) where the vegetation water content was directly
17 related to VOD. The algorithm of the VOD dataset we used here is based on the land
18 parameter retrieval model (LPRM) (Meesters et al., 2005; Owe et al., 2001, 2008). LPRM is
19 based on a radiative transfer model and solves simultaneously for soil moisture and VOD. It
20 can be applied to passive microwave sensors and has been used in numerous studies (see de
21 Jeu et al., 2014). VOD can be used to estimate biomass (Liu et al., 2015), and changes therein
22 correspond to net forest loss (equals the net sum of deforestation, degradation and regrowth)
23 in a 0.25° grid cell.

24 The VOD time series used here is based on merging observations from two sensors (Liu et al.,
25 2011a). The different observations come from SSM/I (1988-2007) and AMSR-E (July 2002-
26 September 2011). These two sensors have different specifications regarding wavelength,
27 viewing angle and spatial footprint and therefore the absolute values of the retrieved VOD
28 values differ. Their relative dynamics, however, are similar (Liu et al., 2011a). In the merging
29 procedure the AMSR-E retrievals were used as a reference, because this product has the
30 higher accuracy due to its relatively low frequency. The cumulative distribution frequency
31 (CDF) matching technique was used for rescaling SSM/I to match AMSR-E. For the period

1 July 2002 through September 2011 AMSR-E data are used. Before July 2002, SSM/I
2 observations are used. Full details on the merging process can be found in Liu et al. (2011a,
3 2011b). In this study, we used monthly values, which were derived from the merged VOD
4 dataset (version January 2015) by averaging the daily data fields, and were resampled to
5 0.25° . VOD observations are dimensionless and their values range from 0 to 1.5. At a certain
6 point, when VOD values exceed 0.8, the vegetation becomes so dense that the soil component
7 in the radiative transfer becomes very small. This is a gradual process and when VOD values
8 are higher than 0.8 additional checks are necessary before using the values in vegetation
9 studies. When VOD exceeds 1.2 smaller scale variations in the vegetation canopy cannot be
10 captured anymore (Owe et al., 2001).

11 **2.2 Global Forest Change (GFC)**

12 Hansen et al. (2013) released early 2014 the Global Forest Change (GFC) project gridded
13 dataset, which is probably the most data rich and computer intensive production of global
14 forest change maps. It contains annual maps over the time period 2001-2013 at a 30-meter
15 resolution. The maps are based on the 30-meter Landsat 7 Enhanced Thematic Mapper Plus
16 (ETM+) scenes, which were resampled and normalized to create a gridded dataset of cloud-
17 free image observations. Forest loss is defined in GFC as a change from forest to non-forest
18 state, comprising deforestation and degradation. In our analysis, we used the annual forest
19 loss dataset and reprocessed these to the 0.25° resolution of our analysis by summing the 30-
20 meter values. While regrowth is detected and reported, we focused on the forest loss data
21 when we used GFC for comparison; regrowth is thus not included in our analysis of GFC. We
22 did not include the 2000 forest cover map as mask for forested areas to avoid omitting areas
23 that were deforested before 2000.

24 **2.3 PRODES deforestation**

25 The Brazilian space agency INPE provides annual gross deforestation maps of the Brazilian
26 Legal Amazon within the Program for Deforestation Assessment in the Brazilian Legal
27 Amazonia (PRODES). INPE defines deforestation as the gross deforestation rate of the
28 conversion of intact forests (old growth forest) to a different land use such as agro-pasture,
29 wood exploration areas and silviculture. Degradation and deforestation of regenerating
30 secondary forests are not monitored by PRODES (INPE, 2013).

1 Although PRODES covers a relatively long time period, the method of detection of
2 deforestation has changed over time. For the time period 1988-2002 the detection of
3 deforestation polygons was done by visual interpretation of Landsat 5 and Landsat 7 scenes.
4 More recently these polygons were manually digitized in the PRODES Analog project (INPE,
5 2013). After 2002, PRODES started to use digital image processing and visual interpretation
6 of Landsat bands 3, 4 and 5 creating and interpreting images of soil, shade and vegetation
7 fractions (INPE, 2013; Shimabukuro et al., 1998). Deforestation is reported once per year in
8 August based on changes over the previous 12-month period. Deforestation within PRODES
9 is defined as clear-cut areas of primary forests exceeding 6.25 ha. Because of this threshold in
10 detection omitting deforestation smaller than 6.25 ha, INPE reports that underestimation of
11 deforestation occurs. Furthermore there may be unobserved areas due to cloud cover in the
12 Landsat images during the time period of visual interpretation until 2005 (INPE, 2013).

13

14 **3 Methods**

15 In this section we will first explain the pre-processing of the data (Sect. 3.1), followed by
16 describing the methodology used to detect forest loss (Sect. 3.2). Finally we will explain how
17 the detected changes were converted to forest loss area (Sect. 3.3)

18 **3.1 Data selection**

19 We aimed to estimate gross forest loss for each 0.25° pixel on an annual basis, which will be
20 explained in Sect. 3.2. We first filtered the available data to circumvent false detections
21 related to the use of microwave data. The excluded grid cells are shown in Fig. 1, and the data
22 exclusion was based on two criteria:

- 23 1. Average VOD values should be below 1.2. This is to prevent false detection in densely
24 vegetated areas without clear forest loss. The value was based on Owe et al (2001),
25 who stated that VOD values larger than 1.2 cannot be used to detect significant
26 vegetation changes. When vegetation is very dense, the VOD signal becomes noisy
27 and potential changes in forest cover cannot be detected anymore. These pixels are
28 mainly found in the middle of the Amazon forest, where forest loss rates are low. In
29 addition, we excluded grid cells where VOD values were on average below 0.6 to
30 maintain a focus on forested grid cells. Also when forest loss occurs in the early stages
31 of the time series, the average VOD value will not be below this limit of 0.6. This

1 value was based on the comparison between VOD and MODIS-based Vegetation
2 Continuous Fields (VCF), which provides information about the fraction tree cover in
3 a pixel. Our VOD threshold of 0.6 corresponds to 10% tree cover for two-third of the
4 pixels, a percentage sometimes used to define forest (Saatchi et al., 2011; UNFCCC,
5 2006) although there is no consensus about this definition.

- 6 2. Large open water should be avoided. Open water affects microwave emissions and can
7 lead to underestimation of VOD (Jones et al., 2011). Therefore 0.25° grid cells, which
8 contain more than 50% open water based on the Global Lakes and Wetlands Database
9 (GLWD, Lehner and Döll, 2004), were masked out.

10 We excluded these grid cells also from GFC and PRODES data when we compared the
11 results. Therefore, total South American forest loss over 2001-2010 for GFC reported here are
12 on average 4% lower than without the data exclusion, which also gives an indication of our
13 underestimation due to masking out of these grid cells.

14 **3.2 Detection of forest loss**

15 Our method is a change detection method based on the principle that VOD is directly related
16 to the aboveground living biomass. Therefore persistent changes in VOD over time are related
17 to changes in biomass (Liu et al., 2015), for example when forest is converted to non-forest.
18 Basically we track the full time series and inspect whether there are sudden drops in the signal
19 that could be the result of forest loss. Our approach is based on 4 steps and explained using an
20 example grid cell located in the Brazilian state of Mato Grosso, where forest loss has been
21 high during the 2000-2005 interval according to Hansen et al. (2010).

22 As a first step we deseasonalized the time series based on a 19-month moving average of
23 VOD ($VOD_{MovingAVG}$, Fig. 2a):

$$24 \quad VOD_{MovingAVG}(lat, lon, m) = Average(VOD_{obs}(lat, lon, m - 9 : m + 9)) \quad (1)$$

25 where lat, lon, m is the latitude (lat), longitude (lon) and month (m). With $m-9:m+9$ we refer to
26 all data points 9 months before until 9 months after the specific month. This approach was
27 preferred over taking out the seasonal cycle based on the average of all cycles because the
28 seasonal cycle from forest and non-forest is different. In addition, a longer moving average
29 masks part of the signal due to droughts or anomalous wet periods which also influence VOD.
30 We also tested longer averaging windows (See Sect. 4.5 for details about the tested windows),

1 but the results were relatively insensitive to this and it decreased the numbers of years over
2 which we could report. In the example grid cell $VOD_{MovingAVG}$ decreased most strongly during
3 2002-2005 (Fig. 2a).

4 To estimate where forest loss potentially occurred and how this was partitioned over different
5 year(s), in the second step we calculated the difference of $VOD_{MovingAVG}$ with the same
6 variable 12 months earlier, and label this the inter-yearly-difference (IYD , Fig. 2b):

$$7 \quad IYD(lat, lon, m) = VOD_{MovingAVG}(lat, lon, m) - VOD_{MovingAVG}(lat, lon, m - 12) \quad (2)$$

8 When the IYD was below 0, this specific month was detected as possible moment for forest
9 loss. In the third step, we tested using a two-sided t-test whether IYD was negative because of
10 forest loss, or because of other reasons, for example due to natural interannual variability
11 related to rainfall. The first group of the t-test consisted of all VOD observations preceding
12 the month where IYD was negative. The second group consisted of all other VOD
13 observations from that moment until the end of the time series. When the p -value was smaller
14 than 0.05, we flagged the grid cell and month as forest loss (Fig. 2b). These three steps were
15 done for every grid cell and month from October 1989 until January 2011.

16 In the fourth and final step, we calculated the sum of the absolute IYD values to which we will
17 refer to as $VOD_{outliers}$ in the rest of this paper. This was done from 1990 through 2010 to get
18 annual values (Fig. 2b).

19 **3.3 Conversion to area forest loss**

20 Our method yields the number of $VOD_{outliers}$ per year for each grid cell, which is related
21 qualitatively to the amount of forest loss and may thus yield insight into the spatial and
22 temporal dynamics of forest loss. However, to go one step further and convert our results to
23 the area of forest loss we calibrated our results to the gross forest loss estimates of GFC.
24 Because of the large differences in spatial resolution (30 meter for GFC and 0.25° for VOD)
25 and because our dataset is most useful for large-scale assessments, we calibrated the
26 conversion of the $VOD_{outliers}$ to area based on a country-level approach for the overlapping
27 time period (2001 – 2010). In general, our method yields net forest loss per gridcell within
28 one year, because we considered decreases in VOD, which is the net result of deforestation,
29 forest degradation and regrowth within a gridcell per year.

1 Because VOD and biomass are not linearly related, we binned VOD in 5 groups comprising
2 the average VOD values between 0.6 and 1.2 (0.6-0.7, 0.7-0.8, 0.8-0.9, 0.9-1.0 and 1.0-1.2).
3 The last bin was larger to arrive at more robust regression outcomes, because there are fewer
4 grid cells with VOD above 1.0. For every bin we performed a Pearson regression (Pearson
5 performed preferably, compared to Spearman) forced through the origin, with all $VOD_{outliers}$
6 per year related to the same GFC values. Based on the linear regression, we obtained a slope
7 for each VOD bin, which was used to convert $VOD_{outliers}$ to gross forest loss area per 0.25°
8 grid cell (Eq. 3).

$$9 \quad VOD_{areaforestloss}(year) = \sum_{bin=1}^5 VOD_{outliers}(year, bin) \times slope(bin) \quad (3)$$

10

11 **4 Results**

12 **4.1 Spatial extent**

13 The largest feature over our study period is the well-known arc of deforestation along the
14 Southern edge of the Amazon basin (Fig. 3), showing high forest loss in every period. Highest
15 forest loss was observed in the Brazilian states Mato Grosso, Pará and Maranhão. However,
16 forest loss rates were not uniform in space and time, Fig. 3 shows that forest loss rates have
17 fluctuated with lowest forest loss observed during the 1995-1999 period and the highest forest
18 loss observed over 2000-2004 period.

19 While forest loss in South America is most often associated with this arc of deforestation, also
20 other regions experienced forest loss. One is the region extending from Northern Argentina to
21 Bolivia via Paraguay (Fig. 3a, label 1), also known as the Chaco region, showing high forest
22 loss over the full time period. Forest loss in this region are expanding and increasing in
23 intensity over time. Another region extends from the south eastern part of Paraguay into
24 Brazil along the border of the Brazilian state Mato Grosso do Sul (Fig. 3a, label 2). During
25 the 1995-1999 period forest loss was on the rise here and increased to a maximum during the
26 2000-2004 period, but decreased during the 2005-2009 epoch.

27 Finally, the region north of Manaus in the Brazilian states of Roraima and Amazonas (Fig. 3a,
28 label 3) which partly consists of wooded savanna, also showed high forest loss. Here the
29 forest loss increased and expanded during the 1990s with the biggest change between the first
30 and second half of the 1990s. Forest loss stayed relatively stable during the first half of the

1 00s. During the 2005-2009 time window some areas with intense forest loss in previous
2 periods did not show up anymore, for example large parts of the arc of deforestation. Besides
3 these three large regions, several smaller fluctuations occurred. These can mostly be seen in
4 the south eastern Brazilian state Minas Gerais.

5 **4.2 Calibration with GFC**

6 We converted the summed $VOD_{outliers}$ to a forest loss area according to Eq. 3, where the slopes
7 varied between the 5 different bins (Table 1). The Pearson correlation on a grid-scale was
8 lowest ($r^2=0.52$) for the bin with the average VOD from 0.6-0.7. The other 4 bins had
9 correlations ranging from $r^2=0.63$ to 0.80 (Table 1). The largest errors are found in the regions
10 with dense vegetation and relatively little forest loss (Fig. 4, Fig. 5). The RMSE on a grid-cell
11 scale shows that the bin with the lowest average VOD values (0.6-0.7) has the highest error
12 compared to GFC (Table 1).

13 On a country-scale the correlations per bin were higher with the lowest ($r^2=0.63$) again for the
14 bin with the lowest average VOD (0.6-0.7) and the 4 other bins had increasing correlations
15 from $r^2=0.84$ to 0.96 (Table 1). The country-level comparison of our $VOD_{outliers}$ with GFC
16 forest loss had a Pearson linear agreement of $r^2=0.90$ ($p<0.001$). In Fig. 6 the country-level
17 VOD and GFC forest loss area estimates are plotted against each other along with the 1:1 line.
18 Most data points were reasonably close to this line, although VOD overpredicted forest loss
19 towards the lower end of the spectrum. Especially in the countries with the lowest forest loss,
20 including Surinam, Uruguay, French Guiana and Guyana, our method yielded more forest
21 loss than GFC. As a percentage of the available area per country (Table 2) Uruguay (0.65%),
22 Surinam (0.22%), French Guiana (0.14%) and Guyana (0.13%) also showed higher average
23 forest loss over the overlapping time period based on VOD. Chile is on the other hand the
24 country where VOD provides lower forest loss estimates for the overlapping time period (-
25 0.18%) compared to GFC. The country with the largest relative forest loss is Paraguay for
26 both VOD (1.05%) and GFC (0.98%). In Fig. 7 we show these derived annual forest loss from
27 VOD for the full time period, along with GFC for 2001 through 2010. Obviously the average
28 forest loss area for the overlapping period agrees between both datasets because our approach
29 was tuned to match GFC, but the spatial and temporal variability can be different potentially
30 yielding new insights.

1 The main differences between VOD and GFC are thus that VOD estimates higher forest loss
2 for the countries Uruguay, Paraguay and Chile compared to GFC. Furthermore, although
3 VOD and GFC agreed on Brazil being the main driver of South American forest loss (54% for
4 VOD and 68% for GFC), VOD estimates higher interannual variability in this. This is mainly
5 the case in 2001, 2006 and 2009, where VOD estimated 36%-41% less Brazilian forest loss
6 compared to GFC (Table 2).

7 The main feature in the GFC time series is the peak in 2004 (with values of 49 and 58
8 thousand $\text{km}^2\text{yr}^{-1}$ for GFC and VOD respectively). VOD also shows this peak, but indicates
9 that the two preceding years were high as well, making for a broader peak (2002-2004) with
10 comparable values. The higher VOD values in 2002 and 2003 than GFC were mainly the
11 result from higher estimated forest loss in Argentina and Paraguay. From 2005 onwards both
12 datasets agreed on the decreasing forest loss rates and the interruptions in 2007, 2008 and
13 2010, although the exact patterns differed.

14 Following Brazil, the countries with the highest forest loss were Argentina, Bolivia, Colombia
15 and Paraguay, each responsible for 5-8% of total South American forest loss. The difference
16 between VOD and GFC in relative contribution of each country to the total South American
17 forest loss is on average 2% with the maximum difference of 13% for Brazil (all absolute
18 differences, see Table 2).

19 **4.3 Country-level trends**

20 **4.3.1 2001-2010**

21 To further compare VOD with GFC, we also calculated the trends per country, based on
22 linear regression, over the 2001-2010 period in absolute values and as a percentage relative to
23 their average forest loss over that time period (Table 2). It should be noted that not all the
24 trends are statistically significant, partly because of the large interannual variability (Fig. 7,
25 Table 2). The overall trend for all South American forest loss over the overlapping time
26 period is negative for both datasets with a relative slope of -2.9 and -1.4 % yr^{-2} , for VOD and
27 GFC respectively, which in absolute terms corresponds to -1121 $\text{km}^2\text{yr}^{-2}$ and -568 $\text{km}^2\text{yr}^{-2}$.
28 For individual countries in general both datasets agreed and these trends were highly variable
29 (Table 2).

1 4.3.2 1990-2010

2 Focusing on the full time series, Fig. 7 indicates that total forest loss in South America were
3 not stable or monotonically in- or decreasing. Instead, they appear to be highly dynamic -at
4 least from a VOD perspective-, especially during the first few years of our study period
5 (1990-1994). After that, forest loss was fluctuating without a clear trend until about 2001,
6 with 1991, 1995 and 1999 being high forest loss years. After this fluctuating stage a period
7 with relatively high forest loss started, with 2002-2005 being 4 subsequent years with high
8 forest loss. After 2005 forest loss decreased, with interruptions in 2007 and 2010 (Fig. 7).

9 We calculated the linear trends over the whole time period and the two decades 1990-2000
10 and 2000-2010 separately (Table 3). Over 1990-2010 Uruguay showed a clear relative
11 increasing trend of almost 7% yr⁻² (in absolute values 60 km²yr⁻²). Over the same time period
12 also Argentina, Chile, Paraguay and Venezuela showed substantial in- or decreasing trends
13 larger than 3% yr⁻². When investigating the decades 1990-2000 and 2000-2010 separately,
14 additional patterns emerged. During the 1990s Argentina, Brazil, Colombia, Ecuador and
15 Uruguay had trends exceeding 5% yr⁻². During the 2000s, Brazil, Ecuador and Surinam
16 showed trends below -5% yr⁻². The strongest differences per decade were found in Brazil
17 (where the forest loss trend changed from +9.8% yr⁻² in the 1990s to -7% yr⁻² in the 2000s)
18 Colombia (-16.7% yr⁻² to 0.88% yr⁻²) and in Uruguay (+11.9% yr⁻² to -2.1% yr⁻²) (Table 3).
19 Other countries with substantial different trends between the two periods were Argentina
20 5.8% yr⁻² to 3.4% yr⁻²), French Guiana (-3.8% yr⁻² to 6.3% yr⁻²), Peru (-4.6% yr⁻² to 2.4% yr⁻²)
21 and Surinam (-4% yr⁻² to 5.9% yr⁻²).

22 4.4 Brazilian state-level comparison with PRODES

23 In addition to a comparison on country scale, we also compared our results for the Brazilian
24 states within the legal Amazon using the PRODES dataset (Fig. 8). PRODES covers a longer
25 period than GFC, but provides only data for the Legal Amazon. We do not expect PRODES
26 and our dataset to compare perfectly given that PRODES detects only deforestation of
27 primary forests and VOD detects deforestation, degradation and regrowth including forest
28 loss of secondary forest. Nevertheless, the Pearson's r² over the full 21-year time period
29 between these two datasets was 0.60 (p<0.001) with a RMSE of 1.6E3 km²yr⁻¹ on a state-
30 level.

1 Our results show for the Brazilian states a highly dynamic pattern with no steadily in- or
2 decreasing trend (Fig. 8). The most notable difference between both datasets is that VOD
3 suggest that 1991, 1999, 2002 and 2010 were high forest loss years, which PRODES did not
4 show. Furthermore PRODES showed increasing deforestation from 2002 until a peak in 2004,
5 whereas VOD peaked in 2005. While there are substantial differences in the temporal
6 variability in the VOD and PRODES datasets, they do agree on where most forest loss
7 occurred: Pará and Mato Grosso. Combined, these two states were responsible for 69% and
8 61%, for PRODES and VOD respectively, of all Brazilian Legal Amazon deforestation
9 (PRODES) and forest loss (VOD). The total average forest loss in the Legal Amazon from
10 1990 through 2010 (excluding 1993, which is missing in PRODES) was $16.6E3 \text{ km}^2\text{yr}^{-1}$ and
11 $15.2E3 \text{ km}^2\text{yr}^{-1}$ for PRODES and VOD respectively. The states with largest relative
12 differences between VOD forest loss and PRODES deforestation are Amazonas and Roraima,
13 with $1307 \text{ km}^2\text{yr}^{-1}$ and $499 \text{ km}^2\text{yr}^{-1}$ respectively. These regions have little forest loss. The
14 gridded errors for these states for VOD compared with GFC for the overlapping time period
15 are relatively large: 705% and 399 % for Amazonas and Roraima respectively (Fig. 4, Table
16 4).

17 **4.5 Sensitivity Analysis**

18 Our forest loss detection approach was based on several assumptions, and we tested how
19 sensitive our results are to two main assumptions. First we tested whether the way we used
20 the t-test (i.e. group 1 consists of all data until *IYD* is negative and group 2 consists of all data
21 after this moment) is valid, or whether a fixed or smaller time period would capture forest loss
22 better. The main reason to test this is that based on our method, group sizes in the t-test are
23 not equal and group 2 could become so large, that recovery of vegetation could have taken
24 place. Therefore we performed the same detection method, but now with the t-test group sizes
25 fixed to 12, 24 or 36 months. This implies that the detectable time period changed to 1990-
26 2010, 1991-2009 and 1992-2008 for the three different group sizes. The results showed for
27 both the country-level analysis and the state-level analysis that our original method (without a
28 fixed time period) yielded the highest correlations with GFC and PRODES. In general we
29 found that correlation decreased with decreasing group sizes.

30 Besides the t-test group sizes, we also tested whether excluding grid cells that were not
31 normally distributed would make a difference. This was done because a t-test requires
32 normally distributed data. We tested three scenarios.

- 1 1. The standard scenario, where we excluded grid cells where the total average VOD was
2 either larger than 1.2 or below 0.6, and GLWD was larger than 50%.
- 3 2. As 1., but we also excluded grid cells that were not normally distributed ($p=0.10$).
- 4 3. As 1., but we also excluded grid cells that were not normally distributed ($p=0.05$)

5 Excluding these not-normally distributed grid cells in scenario 2 and 3 implied that
6 respectively 25% and 32% of the total South American forest loss based on GFC would be
7 missed. However, the Pearson's r^2 for all three scenarios stayed 0.90. Based on these results
8 we assumed that excluding the not-normally distributed points did not have an effect on the
9 large-scale country-level analysis and we used all grid cells based on scenario 1 in our
10 analysis.

11 12 **5 Discussion**

13 Our results indicated that the patterns of forest loss change over both space and time, although
14 the well-known arc of deforestation remained the single largest feature in South America over
15 our full study period. Our results agree with earlier work showing that forest loss area, and
16 probably also carbon emissions, declined after peaking in the year 2004 (Food and
17 Agriculture Organization of the United Nations, 2010; Macedo et al., 2012; Malhi et al.,
18 2008; Nepstad et al., 2009). This decrease in forest loss is observed mainly because Brazil
19 reduced forest loss through a combination of conservation policies (law enforcement,
20 expansion of the governmental protection of the Amazon area and strict control of these
21 enforcement by suspension of credit to landowners violating the rules) and because of
22 changes in prices of agricultural outputs from 2005 onwards (Nepstad et al., 2009).

23 While forest loss in the arc of deforestation, the region around the southern border of Mato
24 Grosso do Sul (Fig. 3a, label 2) and the region around Manaus (Fig 3a, label 3) declined after
25 2004, in the Gran Chaco region (Fig. 3a, label 1) it increased over the time, as shown earlier
26 by Chen et al. (2013). In this region the observed forest loss is in areas where deciduous
27 broadleaf forest (>10 metres tall) with closed canopy is converted to shorter (<10 metres)
28 Chacoan woodlands and agricultural areas (Steininger et al., 2001) and could be related to soy
29 bean production in this region (Boletta et al., 2006; Gasparri and Grau, 2009; Zak et al.,
30 2004). This is in line with our trends and time series (Fig 7, Table 2) where both VOD and
31 GFC show an increasing trend for Argentina over 2001-2010, whereas a decreasing trend over

1 that time period occurred in Brazil (Table 2). One explanation could be relocation of
2 agricultural hotspots because of the strict forest law and effective forest law enforcement
3 within Brazil (Dobrovolski and Rattis, 2014).

4 The spatial pattern of forest loss in Northern Brazil in the states of Amazonas and Roraima
5 (Fig. 3, label 3) can partly be explained by forest fires (Fearnside, 2000); the peak during the
6 1995-2000 time period for example could be caused by the El Niño drought fire events during
7 1997 and 1998 (Barbosa and Fearnside, 1999). This is supported by fire emissions estimates
8 for this region derived from the Global Fire Emissions Database (van der Werf et al., 2010).
9 During these droughts, man-made fires destroyed millions of hectares of fragmented and
10 natural forest (Laurance, 1998). This increase that continued during the 2000s in Amazonas
11 and Roraima is not seen anymore in the country-level time series (Fig. 7), because these
12 changes are relatively small compared to the changes in the arc of deforestation.

13 In the country-level analysis between VOD and GFC the latter indicates higher average South
14 American forest loss, with a difference of $3126 \text{ km}^2 \text{ yr}^{-1}$ or $7.6\% \text{ yr}^{-1}$ of average VOD forest
15 loss. The country with the largest absolute contribution in both datasets is Brazil. In GFC
16 Brazil had a 10% larger contribution to the South American total forest loss than in VOD.
17 This could be caused by the difference in what both GFC and VOD measure. GFC measures
18 gross forest loss while, due to our methodology, VOD yields net forest loss. In areas with
19 much regrowth, VOD will therefore underestimate forest loss compared to GFC. This also has
20 the consequence that VOD is most reliable in areas where deforestation is the dominant
21 change. Another reason could be the different spatial resolutions of both satellite products
22 where both datasets are based on. GFC is based on Landsat, which has a spatial resolution of
23 30 meters and can capture more small-scale forest loss events, which will be missed in our
24 dataset based on VOD with its much coarser 0.25° resolution. The difference in spatial
25 resolution could also be the reason why other countries, such as Chile, show less forest loss
26 and higher interannual variability in VOD than in GFC, and why countries with relatively
27 little forest loss, such as Uruguay, Surinam, French Guiana and Guyana had more forest loss
28 based on VOD (Fig. 6). In Uruguay many forest plantations occur (Suppl. Figure 1, Achard et
29 al., 2014) and the result of these plantations is that forest loss is often of small scale. This in
30 combination with the overestimation of VOD with smaller scale forest loss, could explain
31 why Uruguay shows so much higher values on a country level, although additional research is
32 required to better understand these differences. While we would in general favour GFC over

1 VOD during the overlapping periods for reasons mentioned above, the temporal resolution of
2 VOD is superior to any other dataset for our study period from 1990-2010. For areas with
3 frequent cloud cover where Landsat may have difficulties in acquiring reliable data, VOD
4 may be in a better position to map forest loss.

5 We also compared our results for the whole time period from 1990 through 2010 with
6 PRODES data in a state-level comparison and they had a Pearson r^2 of 0.66. As mentioned
7 earlier, to some degree the comparison is one of apples and oranges because PRODES
8 provides annual estimates of deforestation in pixels where no deforestation has occurred
9 before, whereas the VOD dataset will give information about deforestation and degradation
10 and potentially regrowth. Although forest loss based on VOD includes degradation and
11 regrowth, PRODES shows on average over the whole time period $1451 \text{ km}^2\text{yr}^{-1}$ ($9.6\% \text{ yr}^{-1}$ of
12 the total average legal Amazon forest loss according to VOD) more deforestation than VOD.
13 This could be caused by the differences in methodology and spatial resolution of both datasets
14 we mentioned before, but also potential inconsistencies in PRODES could play a role; until
15 2002 PRODES is based on visual interpretation, after which PRODES digital was used. On a
16 state-level VOD overestimates forest loss area in the states of Amazonas and Roraima, which
17 is mostly related to the relatively low and small-scale forest loss in these states (Fig. 4, Table
18 4).

19 One of the most striking differences between VOD and PRODES were the years 1991, 1999
20 and 2010 when VOD was much higher than PRODES. The underlying reasons may not be
21 directly related to forest loss. In 1991 this difference could be explained by the eruption of
22 Mount Pinatubo, which had the result that led to increased VOD in the tropics (Kobayashi and
23 Dye, 2005; Liu et al., 2011a). The peak in 1999 in VOD was mainly caused by an increase in
24 the state of Amazonas. During 1999 heavy floodings occurred in this region (Chen et al.,
25 2010). Since VOD is sensitive to large waters, the VOD signal could have been influenced by
26 this event. Finally the peak in 2010 could be caused by drought that hit the Amazon that year
27 (Lewis et al., 2011). Amazon forests are sensitive to increasing moisture stress and this could
28 affect above ground biomass (Phillips et al., 2009). This supports the findings of Liu et al.
29 (2012), who noticed that VOD responded to interannual variability in precipitation for
30 tropical regions. However, this 2010 peak in forest loss was also detected by GFC. PRODES
31 did not show this peak, partly because it was related to secondary forest degradation and
32 deforestation, which is not captured by PRODES (Fanin and van der Werf, 2015). This

1 indicates the need to better reconcile the differences between these various estimates and not
2 rely on one single dataset.

3 **6 Conclusions**

4 We have used a new satellite-based dataset using microwave observations to estimate forest
5 loss in South America for the 1990-2010 period in a consistent manner. Our approach may
6 have difficulties in capturing small-scale forest loss and may be impacted on interannual
7 scales by anomalous dry or wet conditions, and is therefore most useful for regional, long-
8 term assessments. The long study period of our study enabled us to improve on characterizing
9 the spatiotemporal dynamic nature of forest loss. Our results confirm the well-known
10 decrease of forest loss in the Brazilian Amazon since 2005, but indicate no trend over the full
11 time period for our whole study region. In the regions south of the arc of deforestation,
12 however, forest loss has increased over the full time period. This includes Argentina, Bolivia,
13 Chile, and Paraguay where trends up to $4\% \text{ yr}^{-2}$ were observed over 1990-2010, partly
14 offsetting the reductions in forest loss in Brazil.

15 Each of the datasets used here has limitations for mapping forest loss including length of time
16 period (GFC), limited spatial domain and focus on detecting only pristine forest loss
17 (PRODES), and coarse resolution and influence of anomalously dry and wet periods on the
18 detected signal (VOD). This indicates that better understanding the differences between those,
19 and other, forest loss datasets requires more scrutiny and that uncertainties are large when
20 relying on one single dataset. We presented a first attempt towards a better forest loss dataset
21 using VOD to better understand forest loss dynamics. The added value of our analysis is
22 mostly providing new annual forest loss estimates during the 1990s, a period not covered by
23 GFC, MODIS and other satellite datasets. More research is needed to better understand what
24 VOD exactly represents, potentially comparing with existing lidar-based benchmark datasets
25 (Baccini et al., 2012; Saatchi et al., 2011).

26

27 **Acknowledgements**

28 We thank Douglas Morton, Jan Verbesselt and Niels Andela for useful discussions.
29 Furthermore we acknowledge INPE and Matthew Hansen for making their data publicly
30 available. This research was supported by the European Research Council grant number
31 280061.

32

1 **References**

- 2 Achard, F., Beuchle, R., Mayaux, P., Stibig, H.-J., Bodart, C., Brink, A., Carboni, S., Desclée,
3 B., Donnay, F., Eva, H. D., Lupi, A., Raši, R., Seliger, R. and Simonetti, D.: Determination of
4 tropical deforestation rates and related carbon losses from 1990 to 2010, *Glob. Chang. Biol.*,
5 20, 2540–2554, doi:10.1111/gcb.12605, 2014.
- 6 Andela, N., Liu, Y. Y., van Dijk, A. I. J. M., de Jeu, R. A. M. and McVicar, T. R.: Global
7 changes in dryland vegetation dynamics (1988-2008) assessed by satellite remote sensing:
8 Comparing a new passive microwave vegetation density record with reflective greenness data,
9 *Biogeosciences*, 10, 6657–6676, doi:10.5194/bg-10-6657-2013, 2013.
- 10 Anyamba, A. and Tucker, C. J.: Analysis of Sahelian vegetation dynamics using NOAA-
11 AVHRR NDVI data from 1981-2003, in *Journal of Arid Environments*, vol. 63, pp. 596–614.,
12 2005.
- 13 Asner, G. P.: Cloud cover in Landsat observations of the Brazilian Amazon, *Int. J. Remote*
14 *Sens.*, 22, 3855–3862, doi:10.1080/01431160010006926, 2001.
- 15 Baccini, A., Goetz, S. J., Walker, W. S., Laporte, N. T., Sun, M., Sulla-Menashe, D., Hackler,
16 J., Beck, P. S. A., Dubayah, R., Friedl, M. A., Samanta, S. and Houghton, R. A.: Estimated
17 carbon dioxide emissions from tropical deforestation improved by carbon-density maps, *Nat.*
18 *Clim. Chang.*, 2, 182–185, doi:10.1038/nclimate1354, 2012.
- 19 Barbosa, R. I. and Fearnside, P. M.: Incêndios na Amazônia Brasileira: estimativa da emissão
20 de gases do efeito estufa pela queima de diferentes ecossistemas de Roraima na passagem do
21 evento “El Niño” (1997/1998), *Acta Amaz.*, 29, 513–534, 1999.
- 22 Boletta, P. E., Ravelo, A. C., Planchuelo, A. M. and Grilli, M.: Assessing deforestation in the
23 Argentine Chaco, *For. Ecol. Manage.*, 228, 108–114, doi:10.1016/j.foreco.2006.02.045, 2006.
- 24 Broich, M., Hansen, M., Stolle, F., Potapov, P., Margono, B. A. and Adusei, B.: Remotely
25 sensed forest cover loss shows high spatial and temporal variation across Sumatera and
26 Kalimantan, Indonesia 2000–2008, *Environ. Res. Lett.*, 6, 014010, doi:10.1088/1748-
27 9326/6/1/014010, 2011.
- 28 Chen, J. L., Wilson, C. R. and Tapley, B. D.: The 2009 exceptional Amazon flood and
29 interannual terrestrial water storage change observed by GRACE, *Water Resour. Res.*, 46, 1–
30 10, doi:10.1029/2010WR009383, 2010.
- 31 Chen, Y., Morton, D. C., Jin, Y., Collatz, G. J., Kasibhatla, P. S., van der Werf, G. R.,
32 DeFries, R. S. and Randerson, J. T.: Long-term trends and interannual variability of forest,
33 savanna and agricultural fires in South America, *Carbon Manag.*, 4, 617–638,
34 doi:10.4155/cmt.13.61, 2013.
- 35 Costa, M. H. and Foley, J. A.: A comparison of precipitation datasets for the Amazon Basin,
36 *Geophys. Res. Lett.*, 25, 155, doi:10.1029/97GL03502, 1998.
- 37 Dobrovolski, R. and Rattis, L.: Brazil should help developing nations to foster agriculture and
38 environmental protection, *Front. Ecol. Environ.*, 12, 376–376, doi:10.1890/14.WB.010, 2014.
- 39 Ernst, C., Mayaux, P., Verhegghen, A., Bodart, C., Christophe, M. and Defourny, P.: National
40 forest cover change in Congo Basin: Deforestation, reforestation, degradation and
41 regeneration for the years 1990, 2000 and 2005, *Glob. Chang. Biol.*, 19, 1173–1187,
42 doi:10.1111/gcb.12092, 2013.

- 1 Eva, H. D., Achard, F., Beuchle, R., de Miranda, E., Carboni, S., Seliger, R., Vollmar, M.,
2 Holler, W. a., Oshiro, O. T., Arroyo, V. B. and Gallego, J.: Forest cover changes in tropical
3 south and Central America from 1990 to 2005 and related carbon emissions and removals,
4 *Remote Sens.*, 4, 1369–1391, doi:10.3390/rs4051369, 2012.
- 5 Fanin, T. and van der Werf, G. R.: Relationships between burned area, forest cover loss, and
6 land cover change in the Brazilian Amazon based on satellite data, *Biogeosciences*, 12, 6033–
7 6043, doi:10.5194/bg-12-6033-2015, 2015.
- 8 FAO: Global Forest Resources Assessment 2005: Progress towards sustainable forest
9 management, Food and Agricultural Organization of the United Nations, Rome., 2006.
- 10 Fearnside, P. M.: Global Warming and Tropical Land-Use Change: Greenhouse Gas
11 Emissions from Biomass Burning, Decomposition and Soils in Forest Conversion, Shifting
12 Cultivation and Secondary Vegetation, *Clim. Change*, 46, 115–158,
13 doi:10.1023/A:1005569915357, 2000.
- 14 Fearnside, P. M.: Deforestation in Brazilian Amazonia: History, Rates, and Consequences,
15 *Conserv. Biol.*, 19, 680–688, doi:10.1111/j.1523-1739.2005.00697.x, 2005.
- 16 Food and Agriculture Organization of the United Nations: Global forest resources
17 assessments main report, *FAO For. Pap.*, 163 [online] Available from:
18 <http://www.fao.org/docrep/013/i1757e/i1757e00.htm> (Accessed 10 September 2014), 2010.
- 19 Froking, S., Hagen, S., Milliman, T., Palace, M., Shimbo, J. Z. and Fahnestock, M.:
20 Detection of Large-Scale Forest Canopy Change in Pan-Tropical Humid Forests 2000–2009
21 With the SeaWinds Ku-Band Scatterometer, *IEEE Trans. Geosci. Remote Sens.*, 50, 2603–
22 2617, doi:10.1109/TGRS.2011.2182516, 2012.
- 23 Gasparri, N. I. and Grau, H. R.: Deforestation and fragmentation of Chaco dry forest in NW
24 Argentina (1972–2007), *For. Ecol. Manage.*, 258, 913–921, doi:10.1016/j.foreco.2009.02.024,
25 2009.
- 26 Geist, H. J. and Lambin, E. F.: Proximate Causes and Underlying Driving Forces of Tropical
27 Deforestation, *Bioscience*, 52, 143, doi:10.1641/0006-
28 3568(2002)052[0143:PCAUDF]2.0.CO;2, 2002.
- 29 Grainger, A.: Difficulties in tracking the long-term global trend in tropical forest area., *Proc.*
30 *Natl. Acad. Sci. U. S. A.*, 105, 818–23, doi:10.1073/pnas.0703015105, 2008.
- 31 Grau, H. R., Gasparri, N. I. and Aide, T. M.: Agriculture expansion and deforestation in
32 seasonally dry forests of north-west Argentina, *Environ. Conserv.*, 32, 140,
33 doi:10.1017/S0376892905002092, 2005.
- 34 Guan, K., Wood, E. F. and Caylor, K. K.: Multi-sensor derivation of regional vegetation
35 fractional cover in Africa, *Remote Sens. Environ.*, 124, 653–665,
36 doi:10.1016/j.rse.2012.06.005, 2012.
- 37 Hansen, M. C., Potapov, P. V., Moore, R., Hancher, M., Turubanova, S. A., Tyukavina, A.,
38 Thau, D., Stehman, S. V., Goetz, S. J., Loveland, T. R., Kommareddy, A., Egorov, A., Chini,
39 L., Justice, C. O. and Townshend, J. R. G.: High-resolution global maps of 21st-century forest
40 cover change., *Science*, 342, 850–3, doi:10.1126/science.1244693, 2013.
- 41 Hansen, M. C., Stehman, S. V. and Potapov, P. V.: Quantification of global gross forest cover
42 loss., *Proc. Natl. Acad. Sci. U. S. A.*, 107, 8650–8655, doi:10.1073/pnas.0912668107, 2010.

- 1 Harris, N. L., Brown, S., Hagen, S. C., Saatchi, S. S., Petrova, S., Salas, W., Hansen, M. C.,
2 Potapov, P. V and Lotsch, A.: Baseline map of carbon emissions from deforestation in
3 tropical regions., *Science*, 336, 1573–6, doi:10.1126/science.1217962, 2012.
- 4 INPE: PRODES - Metodologia para o Cálculo da Taxa Anual de Desmatamento na Amazônia
5 Legal. [online] Available from: http://www.obt.inpe.br/prodes/metodologia_TaxaProdes.pdf,
6 2013.
- 7 Jackson, T. J. and Schmugge, T. J.: Vegetation effects on the microwave emission of soils,
8 *Remote Sens. Environ.*, 36, 203–212, doi:10.1016/0034-4257(91)90057-D, 1991.
- 9 de Jeu, R. A. M., Holmes, T. R. H., Parinussa, R. M. and Owe, M.: A spatially coherent
10 global soil moisture product with improved temporal resolution, *J. Hydrol.*, 516, 284–296,
11 doi:10.1016/j.jhydrol.2014.02.015, 2014.
- 12 Jones, M. O., Jones, L. A., Kimball, J. S. and McDonald, K. C.: Satellite passive microwave
13 remote sensing for monitoring global land surface phenology, *Remote Sens. Environ.*, 115,
14 1102–1114, doi:10.1016/j.rse.2010.12.015, 2011.
- 15 de Jong, R., Verbesselt, J., Zeileis, A. and Schaepman, M. E.: Shifts in global vegetation
16 activity trends, *Remote Sens.*, 5, 1117–1133, doi:10.3390/rs5031117, 2013.
- 17 Joshi, N., Mitchard, E. T., Woo, N., Torres, J., Moll-Rocek, J., Ehammer, A., Collins, M.,
18 Jepsen, M. R. and Fensholt, R.: Mapping dynamics of deforestation and forest degradation in
19 tropical forests using radar satellite data, *Environ. Res. Lett.*, 10, 034014, doi:10.1088/1748-
20 9326/10/3/034014, 2015.
- 21 Kerr, Y. H. and Njoku, E. G.: Semiempirical model for interpreting microwave emission from
22 semiarid land surfaces as seen from space, *IEEE Trans. Geosci. Remote Sens.*, 28, 384–393,
23 doi:10.1109/36.54364, 1990.
- 24 Kim, D.-H., Sexton, J. O. and Townshend, J. R.: Accelerated deforestation in the humid
25 tropics from the 1990s to the 2000s, *Geophys. Res. Lett.*, 42, 3495–3501,
26 doi:10.1002/2014GL062777, 2015.
- 27 Kirdiashev, K. P., Chukhlantsev, A. A. and Shutko, A. M.: Microwave radiation of the earth's
28 surface in the presence of vegetation cover, *Radio Eng. Electron. Phys.*, 24, 256–264, 1979.
- 29 Kobayashi, H. and Dye, D. G.: Atmospheric conditions for monitoring the long-term
30 vegetation dynamics in the Amazon using normalized difference vegetation index, *Remote
31 Sens. Environ.*, 97, 519–525, doi:10.1016/j.rse.2005.06.007, 2005.
- 32 Koh, L. P., Miettinen, J., Liew, S. C. and Ghazoul, J.: Remotely sensed evidence of tropical
33 peatland conversion to oil palm., *Proc. Natl. Acad. Sci. U. S. A.*, 108, 5127–32,
34 doi:10.1073/pnas.1018776108, 2011.
- 35 Laurance, W. F.: A crisis in the making: Responses of Amazonian forests to land use and
36 climate change, *Trends Ecol. Evol.*, 13, 411–415, doi:10.1016/S0169-5347(98)01433-5, 1998.
- 37 Lehner, B. and Döll, P.: Development and validation of a global database of lakes, reservoirs
38 and wetlands, *J. Hydrol.*, 296, 1–22, doi:10.1016/j.jhydrol.2004.03.028, 2004.
- 39 Lewis, S. L., Brando, P. M., Phillips, O. L., van der Heijden, G. M. F. and Nepstad, D.: The
40 2010 Amazon drought., *Science*, 331, 554, doi:10.1126/science.1200807, 2011.
- 41 Liu, Y. Y., van Dijk, A. I. J. M., de Jeu, R. A. M., Canadell, J. G., McCabe, M. F., Evans, J.
42 P. and Wang, G.: Recent reversal in loss of global terrestrial biomass, *Nat. Clim. Chang.*, 5,

- 1 470–474, doi:10.1038/nclimate2581, 2015.
- 2 Liu, Y. Y., van Dijk, A. I. J. M., McCabe, M. F., Evans, J. P. and de Jeu, R. A. M.: Global
3 vegetation biomass change (1988–2008) and attribution to environmental and human drivers,
4 *Glob. Ecol. Biogeogr.*, 22, 692–705, doi:10.1111/geb.12024, 2012.
- 5 Liu, Y. Y., Evans, J. P., McCabe, M. F., de Jeu, R. A. M., van Dijk, A. I. J. M., Dolman, A. J.
6 and Saizen, I.: Changing climate and overgrazing are decimating Mongolian steppes., *PLoS*
7 *One*, 8, e57599, doi:10.1371/journal.pone.0057599, 2013.
- 8 Liu, Y. Y., de Jeu, R. A. M., McCabe, M. F., Evans, J. P. and van Dijk, A. I. J. M.: Global
9 long-term passive microwave satellite-based retrievals of vegetation optical depth, *Geophys.*
10 *Res. Lett.*, 38, L18402, doi:10.1029/2011GL048684, 2011a.
- 11 Liu, Y. Y., Parinussa, R. M., Dorigo, W. A., de Jeu, R. A. M., Wagner, W., M. van Dijk, A. I.
12 J., McCabe, M. F. and Evans, J. P.: Developing an improved soil moisture dataset by blending
13 passive and active microwave satellite-based retrievals, *Hydrol. Earth Syst. Sci.*, 15, 425–436,
14 doi:10.5194/hess-15-425-2011, 2011b.
- 15 Macedo, M. N., DeFries, R. S., Morton, D. C., Stickler, C. M., Galford, G. L. and
16 Shimabukuro, Y. E.: Decoupling of deforestation and soy production in the southern Amazon
17 during the late 2000s, *Proc. Natl. Acad. Sci. U. S. A.*, 109, 1341–1346,
18 doi:10.1073/pnas.1111374109, 2012.
- 19 Malhi, Y.: The carbon balance of tropical forest regions, 1990–2005, *Curr. Opin. Environ.*
20 *Sustain.*, 2, 237–244, doi:10.1016/j.cosust.2010.08.002, 2010.
- 21 Malhi, Y., Roberts, J. T., Betts, R. A., Killeen, T. J., Li, W. and Nobre, C. A.: Climate
22 change, deforestation, and the fate of the Amazon., *Science*, 319, 169–172,
23 doi:10.3832/efor0516-005, 2008.
- 24 Mayaux, P., Achard, F. and Malingreau, J.-P.: Global tropical forest area measurements
25 derived from coarse resolution satellite imagery: a comparison with other approaches,
26 *Environ. Conserv.*, 25, 37–52, doi:10.1017/S0376892998000083, 1998.
- 27 Meesters, A. G. C. A., De Jeu, R. A. M. and Owe, M.: Analytical derivation of the vegetation
28 optical depth from the microwave polarization difference index, *IEEE Geosci. Remote Sens.*
29 *Lett.*, 2, 121–123, doi:10.1109/LGRS.2005.843983, 2005.
- 30 Mitchard, E. T. A., Saatchi, S. S., White, L. J. T., Abernethy, K. A., Jeffery, K. J., Lewis, S.
31 L., Collins, M., Lefsky, M. A., Leal, M. E., Woodhouse, I. H. and Meir, P.: Mapping tropical
32 forest biomass with radar and spaceborne LiDAR in Lopé National Park, Gabon: overcoming
33 problems of high biomass and persistent cloud, *Biogeosciences*, 9, 179–191, doi:10.5194/bg-
34 9-179-2012, 2012.
- 35 Mo, T., Choudhury, B. J., Schmugge, T. J., Wang, J. R. and Jackson, T. J.: A model for
36 microwave emission from vegetation-covered fields, *J. Geophys. Res.*, 87, 11229,
37 doi:10.1029/JC087iC13p11229, 1982.
- 38 Morton, D. C., Defries, R. S., Randerson, J. T., Giglio, L., Schroeder, W. and van der Werf,
39 G. R.: Agricultural intensification increases deforestation fire activity in Amazonia, *Glob.*
40 *Chang. Biol.*, 14, 2262–2275, doi:10.1111/j.1365-2486.2008.01652.x, 2008.
- 41 Morton, D. C., DeFries, R. S., Shimabukuro, Y. E., Anderson, L. O., Del Bon Espírito-Santo,
42 F., Hansen, M. and Carroll, M.: Rapid Assessment of Annual Deforestation in the Brazilian
43 Amazon Using MODIS Data, *Earth Interact.*, 9, 1–22, doi:10.1175/EI139.1, 2005.

- 1 Myneni, R. B., Hall, F. G., Sellers, P. J. and Marshak, A. L.: The interpretation of spectral
2 vegetation indexes, *IEEE Trans. Geosci. Remote Sens.*, 33, 481–486, doi:10.1109/36.377948,
3 1995.
- 4 Naylor, R., Steinfeld, H., Falcon, W., Galloway, J., Smil, V., Bradford, E., Alder, J. and
5 Mooney, H.: Agriculture. Losing the links between livestock and land., *Science*, 310, 1621–2,
6 doi:10.1126/science.1117856, 2005.
- 7 Nepstad, D., Soares-Filho, B. S., Merry, F., Lima, A., Moutinho, P., Carter, J., Bowman, M.,
8 Cattaneo, A., Rodrigues, H., Schwartzman, S., McGrath, D. G., Stickler, C. M., Lubowski, R.,
9 Piris-Cabezas, P., Rivero, S., Alencar, A., Almeida, O. and Stella, O.: Environment. The end
10 of deforestation in the Brazilian Amazon., *Science*, 326, 1350–1351,
11 doi:10.1126/science.1182108, 2009.
- 12 Owe, M., de Jeu, R. A. M. and Holmes, T.: Multisensor historical climatology of satellite-
13 derived global land surface moisture, *J. Geophys. Res.*, 113, F01002,
14 doi:10.1029/2007JF000769, 2008.
- 15 Owe, M., de Jeu, R. A. M. and Walker, J. P.: A methodology for surface soil moisture and
16 vegetation optical depth retrieval using the microwave polarization difference index, *IEEE*
17 *Trans. Geosci. Remote Sens.*, 39, 1643–1654, doi:10.1109/36.942542, 2001.
- 18 Pan, Y., Birdsey, R. A., Fang, J., Houghton, R., Kauppi, P. E., Kurz, W. A., Phillips, O. L.,
19 Shvidenko, A., Lewis, S. L., Canadell, J. G., Ciais, P., Jackson, R. B., Pacala, S. W.,
20 McGuire, A. D., Piao, S., Rautiainen, A., Sitch, S. and Hayes, D.: A large and persistent
21 carbon sink in the world's forests., *Science*, 333, 988–993, doi:10.1126/science.1201609,
22 2011.
- 23 Phillips, O. L., Aragão, L. E. O. C., Lewis, S. L., Fisher, J. B., Lloyd, J., López-González, G.,
24 Malhi, Y., Monteagudo, A., Peacock, J., Quesada, C. A., van der Heijden, G., Almeida, S.,
25 Amaral, I., Arroyo, L., Aymard, G., Baker, T. R., Bánki, O., Blanc, L., Bonal, D., Brando, P.,
26 Chave, J., de Oliveira, A. C. A., Cardozo, N. D., Czimczik, C. I., Feldpausch, T. R., Freitas,
27 M. A., Gloor, E., Higuchi, N., Jiménez, E., Lloyd, G., Meir, P., Mendoza, C., Morel, A.,
28 Neill, D. A., Nepstad, D., Patiño, S., Peñuela, M. C., Prieto, A., Ramírez, F., Schwarz, M.,
29 Silva, J., Silveira, M., Thomas, A. S., Steege, H. Ter, Stropp, J., Vásquez, R., Zelazowski, P.,
30 Alvarez Dávila, E., Andelman, S., Andrade, A., Chao, K., Erwin, T., Di Fiore, A., Honorio C,
31 E., Keeling, H., Killeen, T. J., Laurance, W. F., Peña Cruz, A., Pitman, N. C. A., Núñez
32 Vargas, P., Ramírez-Angulo, H., Rudas, A., Salamão, R., Silva, N., Terborgh, J. and Torres-
33 Lezama, A.: Drought sensitivity of the Amazon rainforest., *Science*, 323, 1344–1347,
34 doi:10.1126/science.1164033, 2009.
- 35 Potapov, P. V., Turubanova, S. A., Hansen, M. C., Adusei, B., Broich, M., Altstatt, A., Mane,
36 L. and Justice, C. O.: Quantifying forest cover loss in Democratic Republic of the Congo,
37 2000-2010, with Landsat ETM+ data, *Remote Sens. Environ.*, 122, 106–116,
38 doi:10.1016/j.rse.2011.08.027, 2012.
- 39 Poulter, B., Frank, D., Ciais, P., Myneni, R. B., Andela, N., Bi, J., Broquet, G., Canadell, J.
40 G., Chevallier, F., Liu, Y. Y., Running, S. W., Sitch, S. and van der Werf, G. R.: Contribution
41 of semi-arid ecosystems to interannual variability of the global carbon cycle., *Nature*, 509,
42 600–3, doi:10.1038/nature13376, 2014.
- 43 Saatchi, S. S., Harris, N. L., Brown, S., Lefsky, M., Mitchard, E. T. A., Salas, W., Zutta, B.
44 R., Buermann, W., Lewis, S. L., Hagen, S., Petrova, S., White, L., Silman, M. and Morel, A.:
45 Benchmark map of forest carbon stocks in tropical regions across three continents., *Proc.*

- 1 Natl. Acad. Sci. U. S. A., 108, 9899–9904, doi:10.1073/pnas.1019576108, 2011.
- 2 Shi, J., Jackson, T., Tao, J., Du, J., Bindlish, R., Lu, L. and Chen, K. S.: Microwave
3 vegetation indices for short vegetation covers from satellite passive microwave sensor
4 AMSR-E, *Remote Sens. Environ.*, 112, 4285–4300, doi:10.1016/j.rse.2008.07.015, 2008.
- 5 Shimabukuro, Y. E., Batista, G. T., Mello, E. M. K., Moreira, J. C. and Duarte, V.: Using
6 shade fraction image segmentation to evaluate deforestation in Landsat Thematic Mapper
7 images of the Amazon Region, *Int. J. Remote Sens.*, 19, 535–541,
8 doi:10.1080/014311698216152, 1998.
- 9 Steininger, M. K., Tucker, C. J., Townshend, J. R. G., Killeen, T. J., Desch, A., Bell, V. and
10 Ersts, P.: Tropical deforestation in the Bolivian Amazon, *Environ. Conserv.*,
11 doi:10.1017/S0376892901000133, 2001.
- 12 Tucker, C., Pinzon, J., Brown, M., Slayback, D., Pak, E., Mahoney, R., Vermote, E. and El
13 Saleous, N.: An extended AVHRR 8-km NDVI dataset compatible with MODIS and SPOT
14 vegetation NDVI data, *Int. J. Remote Sens.*, 26, 4485–4498,
15 doi:10.1080/01431160500168686, 2005.
- 16 UNFCCC: Annex to UNFCCC decision 16/CMP.1 Land use, land-use change and forestry,
17 Rep. Conf. Parties Serv. as Meet. Parties to Kyoto Protoc. its first Sess. held Montr. from 28
18 Novemb. to 10 December 2005, FCCC/KP/CM, 3 [online] Available from:
19 <http://unfccc.int/resource/docs/2005/cmp1/eng/08a03.pdf#page=3>, 2006.
- 20 Verbesselt, J., Zeileis, A. and Herold, M.: Near real-time disturbance detection using satellite
21 image time series, *Remote Sens. Environ.*, 123, 98–108, doi:10.1016/j.rse.2012.02.022, 2012.
- 22 Verhegghen, A., Mayaux, P., de Wasseige, C. and Defourny, P.: Mapping Congo Basin
23 vegetation types from 300 m and 1 km multi-sensor time series for carbon stocks and forest
24 areas estimation, *Biogeosciences*, 9, 5061–5079, doi:10.5194/bg-9-5061-2012, 2012.
- 25 Wasige, J. E., Groen, T. A., Smaling, E. and Jetten, V.: Monitoring basin-scale land cover
26 changes in Kagera Basin of Lake Victoria using: Ancillary data and remote sensing, *Int. J.*
27 *Appl. Earth Obs. Geoinf.*, 21, 32–42, doi:10.1016/j.jag.2012.08.005, 2012.
- 28 van der Werf, G. R., Morton, D. C., DeFries, R. S., Giglio, L., Randerson, J. T., Collatz, G. J.
29 and Kasibhatla, P. S.: Estimates of fire emissions from an active deforestation region in the
30 southern Amazon based on satellite data and biogeochemical modelling, *Biogeosciences*, 6,
31 235–249, doi:10.5194/bg-6-235-2009, 2009.
- 32 van der Werf, G. R., Randerson, J. T., Giglio, L., Collatz, G. J., Mu, M., Kasibhatla, P. S.,
33 Morton, D. C., Defries, R. S., Jin, Y. and Van Leeuwen, T. T.: Global fire emissions and the
34 contribution of deforestation, savanna, forest, agricultural, and peat fires (1997-2009), *Atmos.*
35 *Chem. Phys.*, 10, 11707–11735, doi:10.5194/acp-10-11707-2010, 2010.
- 36 Zak, M. R., Cabido, M. and Hodgson, J. G.: Do subtropical seasonal forests in the Gran
37 Chaco, Argentina, have a future?, *Biol. Conserv.*, 120, 589–598,
38 doi:10.1016/j.biocon.2004.03.034, 2004.
- 39 Zhou, L., Tian, Y., Myneni, R. B., Ciais, P., Saatchi, S., Liu, Y. Y., Piao, S., Chen, H.,
40 Vermote, E. F., Song, C. and Hwang, T.: Widespread decline of Congo rainforest greenness
41 in the past decade., *Nature*, 509, 86–90, doi:10.1038/nature13265, 2014.
- 42 Zhu, Z., Bi, J., Pan, Y., Ganguly, S., Anav, A., Xu, L., Samanta, A., Piao, S., Nemani, R. R.
43 and Myneni, R. B.: Global data sets of vegetation leaf area index (LAI)3g and fraction of

1 photosynthetically active radiation (FPAR)3g derived from global inventory modeling and
2 mapping studies (GIMMS) normalized difference vegetation index (NDVI3G) for the period
3 1981 to 2, Remote Sens., 5, 927–948, doi:10.3390/rs5020927, 2013.
4

1 Table 1. Statistics for the comparison between GFC forest loss ($\text{km}^2\text{yr}^{-1}$) and IYD (yr^{-1}). This
 2 was done for all grid cells and when aggregating the grid cells in a country-level analysis. The
 3 coefficient of variation (CV in %) was based on the Root Mean Square Error (RMSE in km^2)
 4 between both datasets.

VOD bin	Based on all grid cells				Country-level		
	slope	r^2	CV (%)	RMSE (km^2)	r^2	CV (%)	RMSE (km^2)
0.6-0.7	22.4	0.63	804	15.7	0.63	203	666
0.7-0.8	34.8	0.52	163	3.7	0.84	122	586
0.8-0.9	61.7	0.80	147	5.0	0.84	83	567
0.9-1.0	79.4	0.72	134	4.7	0.88	92	684
1.0-1.2	82.7	0.72	253	3.2	0.96	53	366

5

- 1 Table 2. Country-level forest loss estimates (total area, contribution to total South American
 2 forest loss, contribution of forest loss as a percentage of the masked-country area, as well as
 3 absolute and relative trends) for VOD and GFC for the overlapping time period (2001-2010).
 4 Asterisks indicate the significance, where *= $p>0.25$ **= $p<0.25$ ***= $p<0.05$

	Average forest loss 2001-2010						Slope 2001-2010			
	Absolute (km ² yr ⁻¹)		Percentage of total forest loss area (Absolute / Total)		Percentage of masked country area (%)		Absolute (km ² yr ⁻²)		Relative (Absolute/Average)	
	VOD	GFC	VOD	GFC	VOD	GFC	VOD	GFC	VOD	GFC
Argentina	4517	3329	11.73%	8.29%	0.61%	0.53%	79*	358**	1.68%	11.00%
Bolivia	3045	2338	8.07%	5.89%	0.39%	0.33%	21*	166***	0.75%	7.84%
Brazil	21926	27317	55.18%	67.81%	0.32%	0.39%	-1385**	-1530**	-6.47%	-5.55%
Chile	173	408	0.50%	1.04%	0.12%	0.30%	35**	17***	18.62%	4.19%
Colombia	1899	1861	4.95%	4.75%	0.20%	0.21%	-2*	65**	-0.13%	3.46%
Ecuador	450	305	1.24%	0.79%	0.18%	0.15%	-63**	19**	-14.19%	6.21%
Fr. Guiana	115	17	0.33%	0.04%	0.16%	0.02%	13**	0*	11.08%	1.18%
Guyana	288	50	0.75%	0.13%	0.16%	0.03%	-3*	0*	-1.24%	-0.61%
Peru	1077	1047	3.06%	2.69%	0.12%	0.13%	52*	84***	4.46%	8.24%
Paraguay	3030	2556	7.68%	6.49%	1.05%	0.98%	115*	213***	3.93%	8.78%
Surinam	276	29	0.75%	0.08%	0.25%	0.03%	34***	2**	12.57%	8.69%
Uruguay	868	122	2.28%	0.31%	0.77%	0.12%	131*	18***	13.61%	15.43%
Venezuela	1322	658	3.46%	1.70%	0.21%	0.11%	-148***	20*	-13.65%	3.12%
Total	38987	40038	100.00%	100.00%			-1121*	-568*	-2.94%	-1.42%

5

6

1 Table 3. Trends in forest loss based on VOD for the whole time period (1990-2010) and the
 2 decades 1990-2000 and 2000-2010. Absolute values indicate the slope based on Pearson
 3 linear regression and the relative values are the absolute values relative to the average forest
 4 loss for that country over the full 21-year time period. Asterisks indicate the significance,
 5 where $*=p>0.25$ $**=p<0.25$ $***=p<0.05$

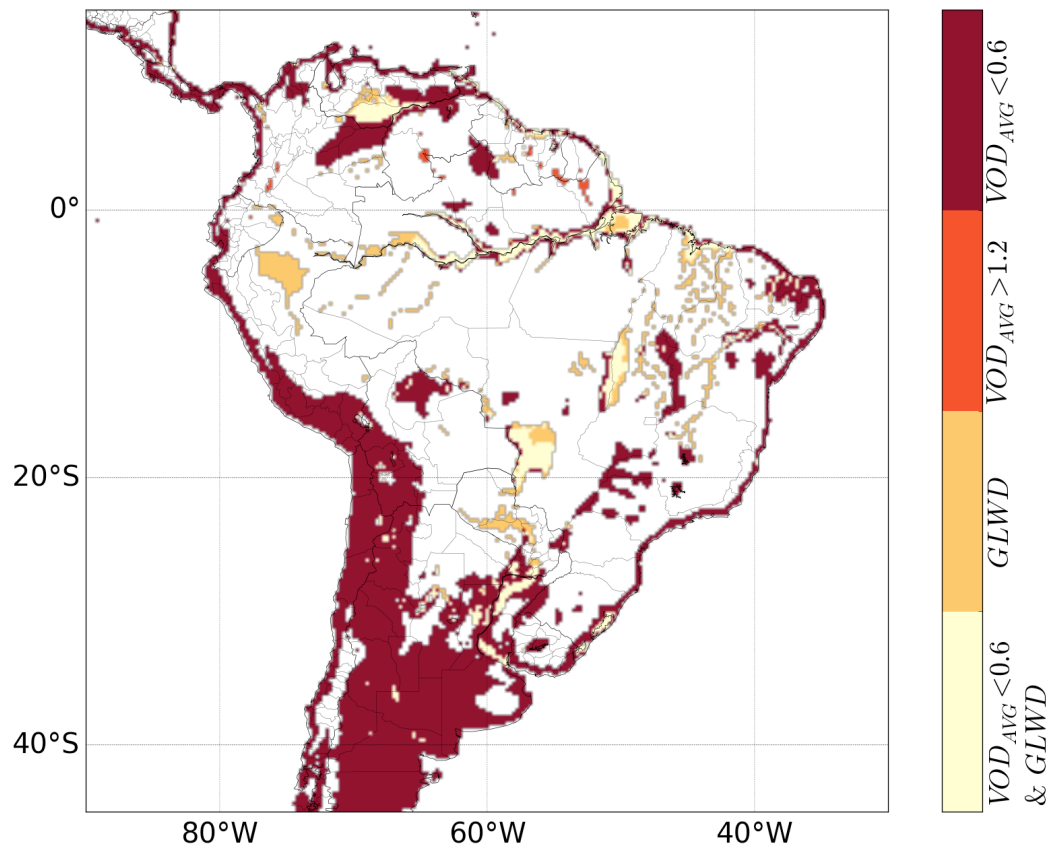
	Slope 1990-2010		Slope 1990-2000		Slope 2000-2010		Difference 00s-90s	
	km ² yr ⁻²	%	km ² yr ⁻²	%	km ² yr ⁻²	%	km ² yr ⁻²	%
Argentina	170***	4.58%	182**	5.76%	109*	3.43%	-73	-2.32%
Bolivia	49**	1.92%	92*	0.75%	72*	0.59%	-20	-0.16%
Brazil	-59*	-0.27%	1078*	9.79%	-765*	-6.95%	-1843	-16.74%
Chile	9**	5.23%	35***	3.34%	23**	2.21%	-12	-1.13%
Colombia	-36*	-1.88%	-197**	-16.69%	10*	0.88%	208	17.57%
Ecuador	-12*	-2.67%	-42**	-14.85%	-35*	-12.58%	6	2.27%
Fr. Guiana	0*	-0.31%	-8*	-3.76%	13***	6.34%	21	10.10%
Guyana	-8**	-2.72%	-16*	-2.12%	4*	0.50%	20	2.61%
Peru	-23*	-1.79%	-85*	-4.55%	45**	2.39%	130	6.94%
Paraguay	98**	3.99%	32*	2.35%	12*	0.86%	-21	-1.49%
Surinam	5*	2.25%	-21**	-4.03%	31***	5.91%	53	9.94%
Uruguay	60***	6.99%	130***	11.91%	-23*	-2.08%	-152	-13.99%
Venezuela	-50***	-3.97%	-57*	-0.30%	-80**	-0.42%	-23	-0.12%
Total	204*	0.55%	1122*	3.01%	-584*	-1.57%	-1706	-4.58%

6

- 1 Table 4. Average error for the Brazilian states. The error is defined as the VOD minus GFC
2 forest loss area expressed as a percentage of GFC forest loss for the overlapping time period
3 per state in the Legal Amazon.

State	(VOD-GFC) / GFC (mean % yr ⁻¹)
Acre	17
Amapá	50
Amazonas	399
Maranhão	17
Mato Grosso	35
Pará	94
Rondônia	37
Roraima	705
Tocantins	2

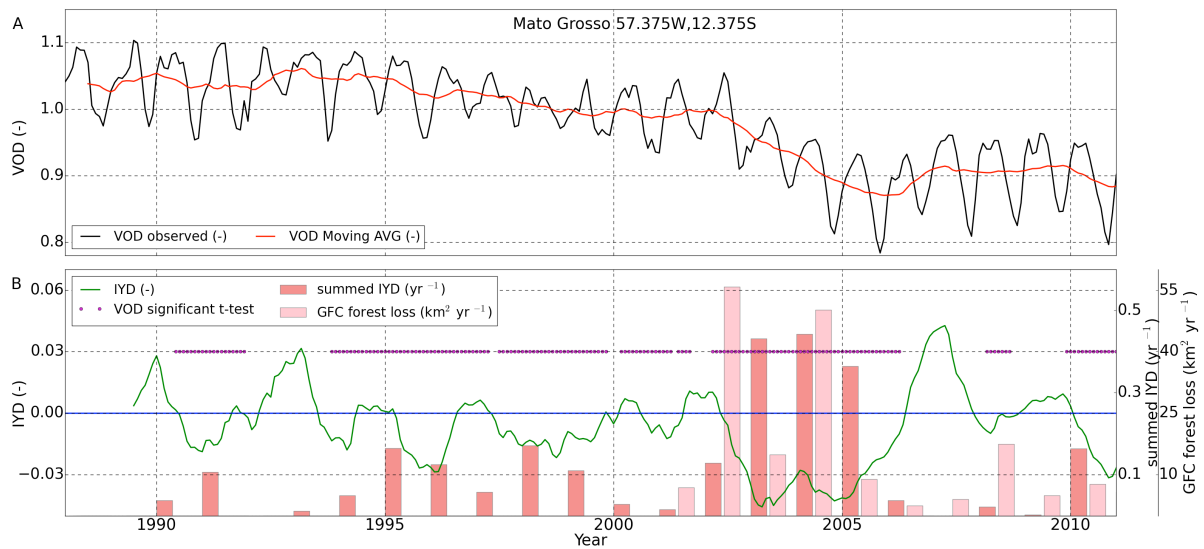
4



1

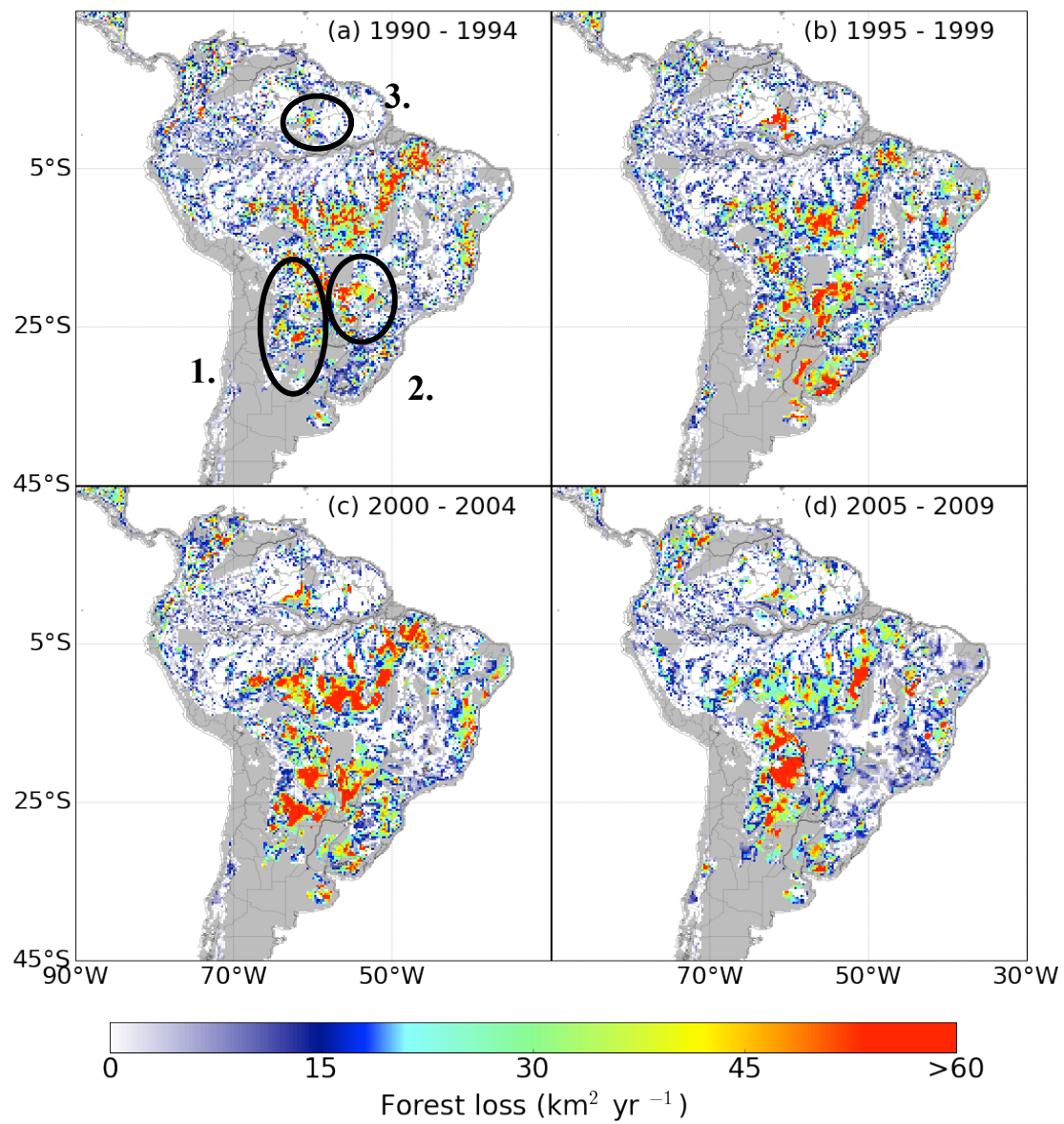
2 Figure 1. Grid cells that were excluded from our analysis: VOD avg: grid cells with an
 3 average VOD that is either above 1.2 or below 0.6 and thus outside the usable range for our
 4 study. GLWD: grid cells containing more than 50% open water, which makes the VOD signal
 5 to become unreliable. Both: grid cells containing more than 50% open water and where VOD
 6 is outside the usable range.

7



1
 2 Figure 2. Example 0.25° grid cell in the Brazilian state of Mato Grosso. A: Observed monthly
 3 VOD signal and 19-month moving average ($VOD_{MovingAVG}$). B: Interyearly difference (IYD),
 4 whether it met the t-test criteria, and annually summed IYD values taking only negative values
 5 into account. For comparison the corresponding GFC values are also given.

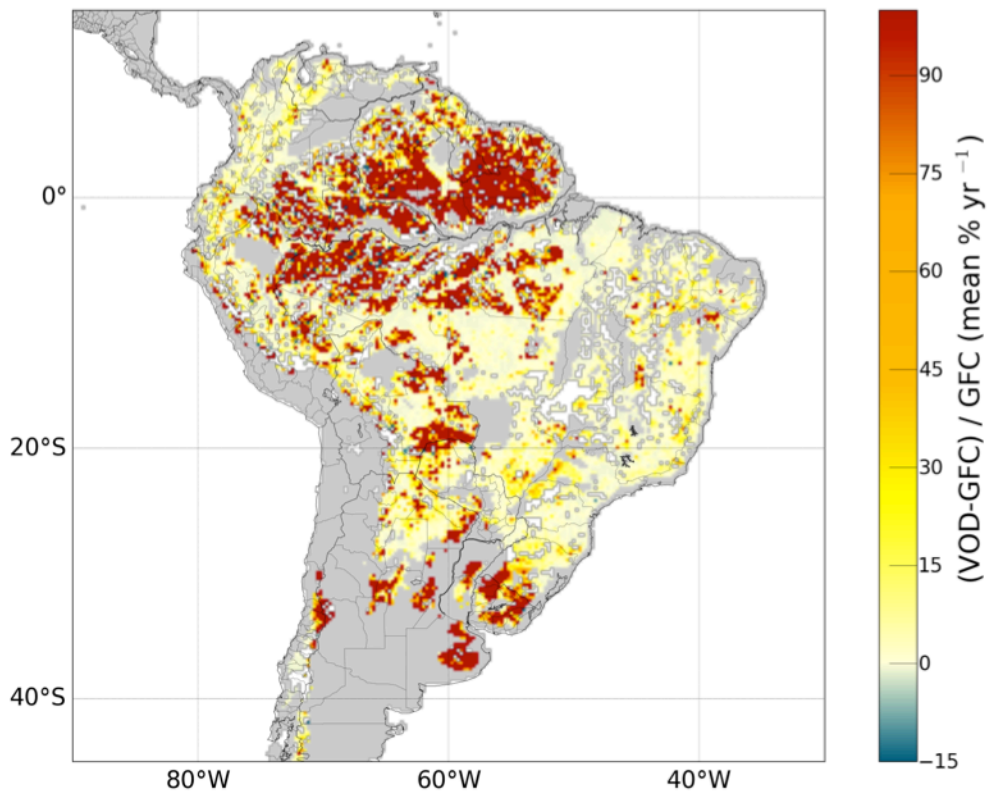
6



1

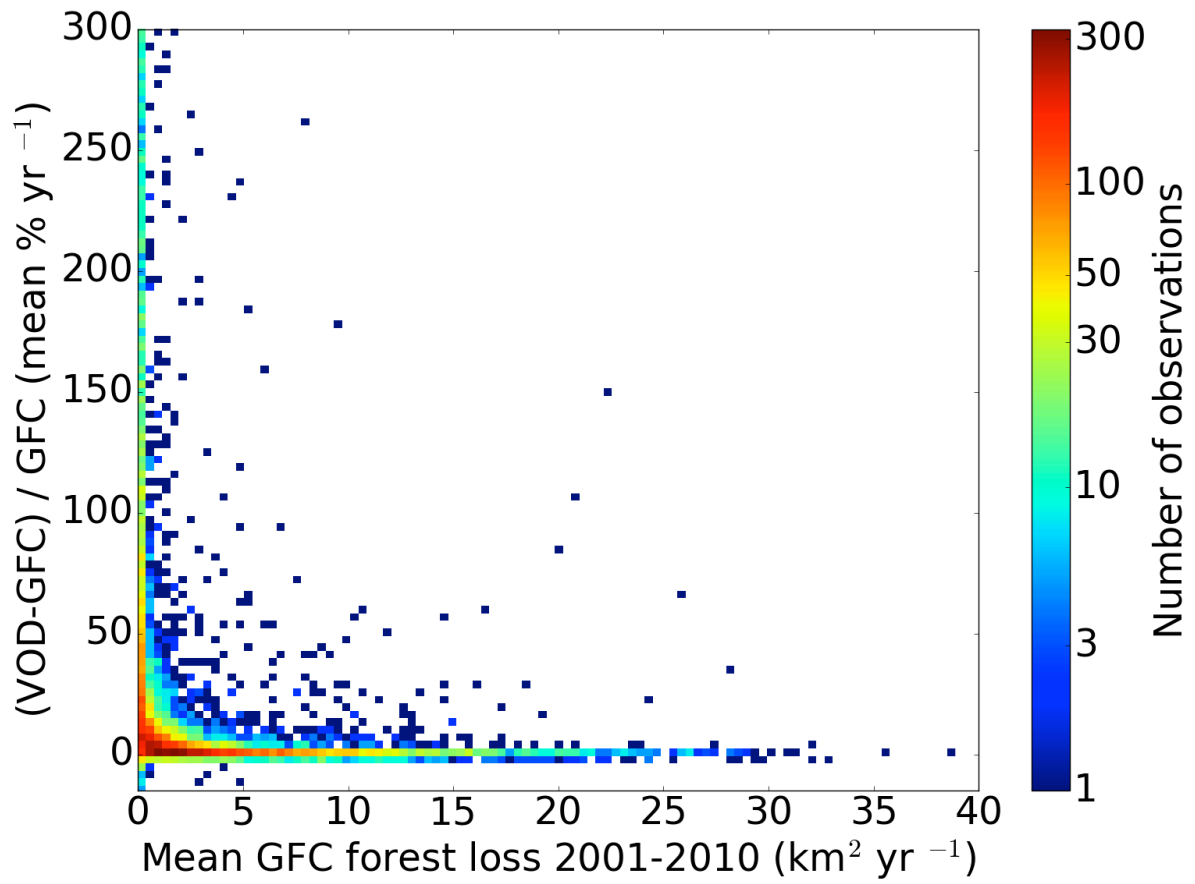
2 Figure 3. Forest loss extent based on the $VOD_{outliers}$ for the 5-year epochs. Grey areas are
 3 masked out (Fig. 1).

4



1
2
3
4
5

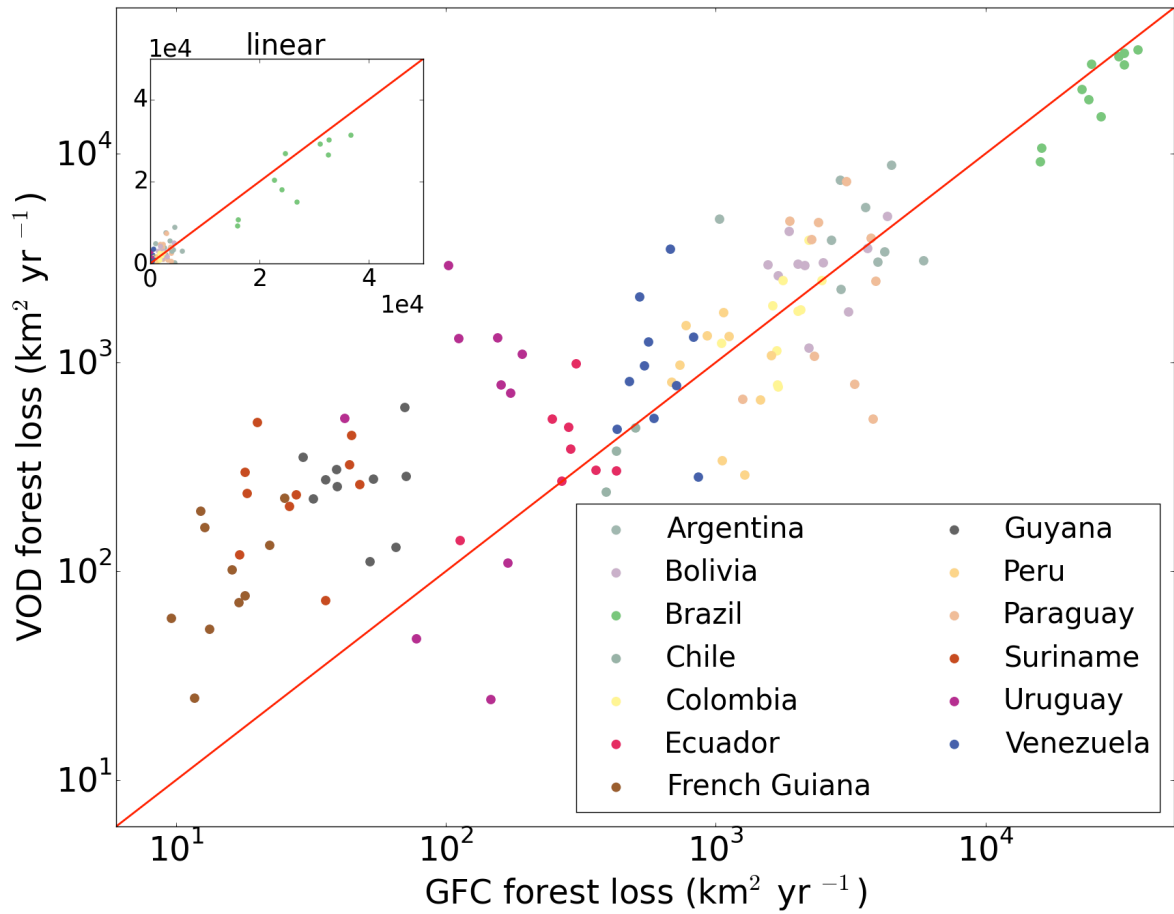
Figure 4. Error estimates for each grid cell. The error is defined as VOD minus GFC forest loss area expressed as a percentage of GFC for the overlapping time period. White indicates that both datasets had no forest loss.



1

2 Figure 5. Error as a function of mean GFC forest loss, where the error is defined as VOD
 3 minus GFC forest loss area as a percentage of GFC for the overlapping time period.

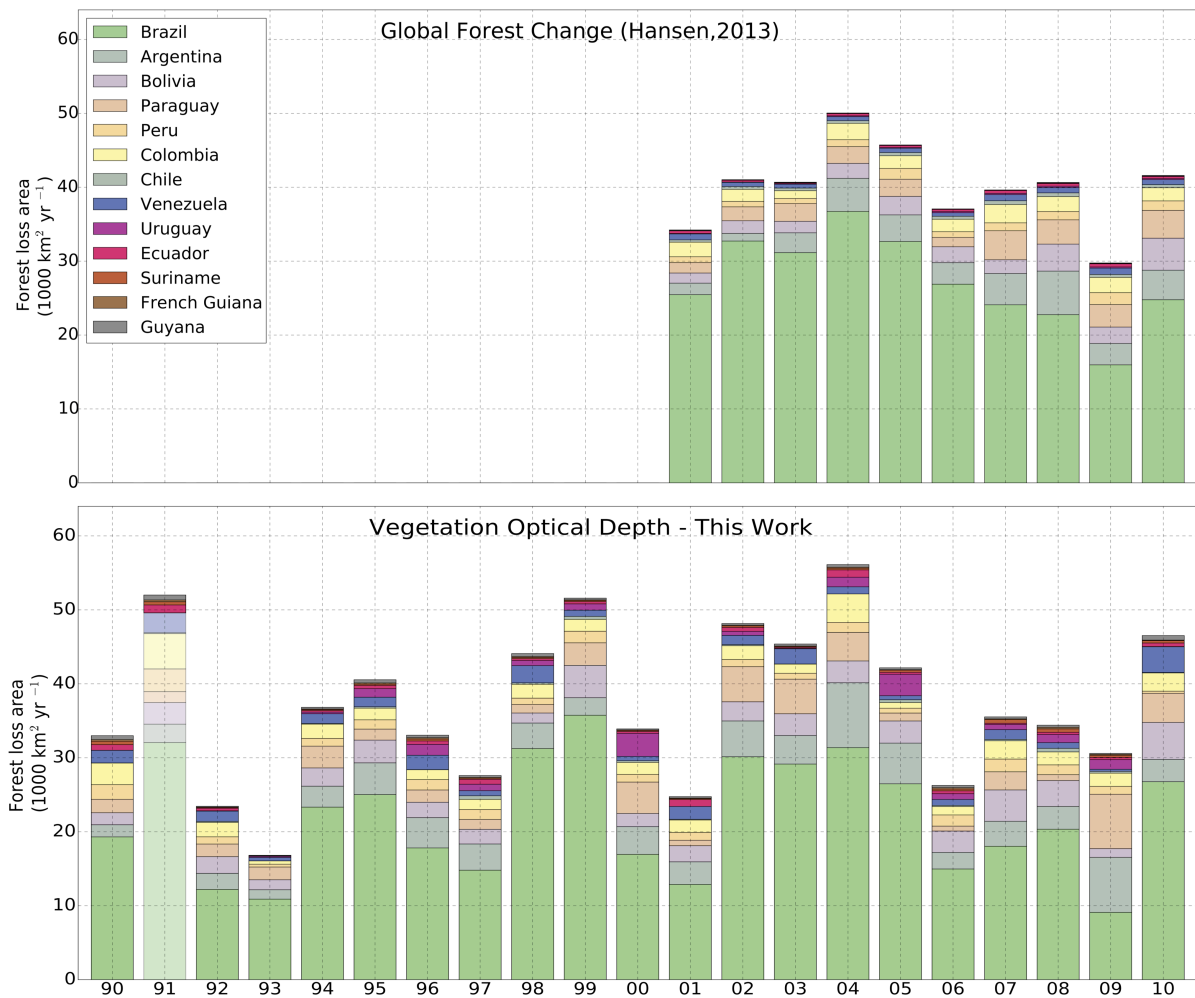
4



1

2 Figure 6. Country-level comparison of calibrated VOD and GFC forest loss based on annual
 3 totals (2001 - 2010). The inset shows the same data on a linear scale. The red lines depict the
 4 1:1 line.

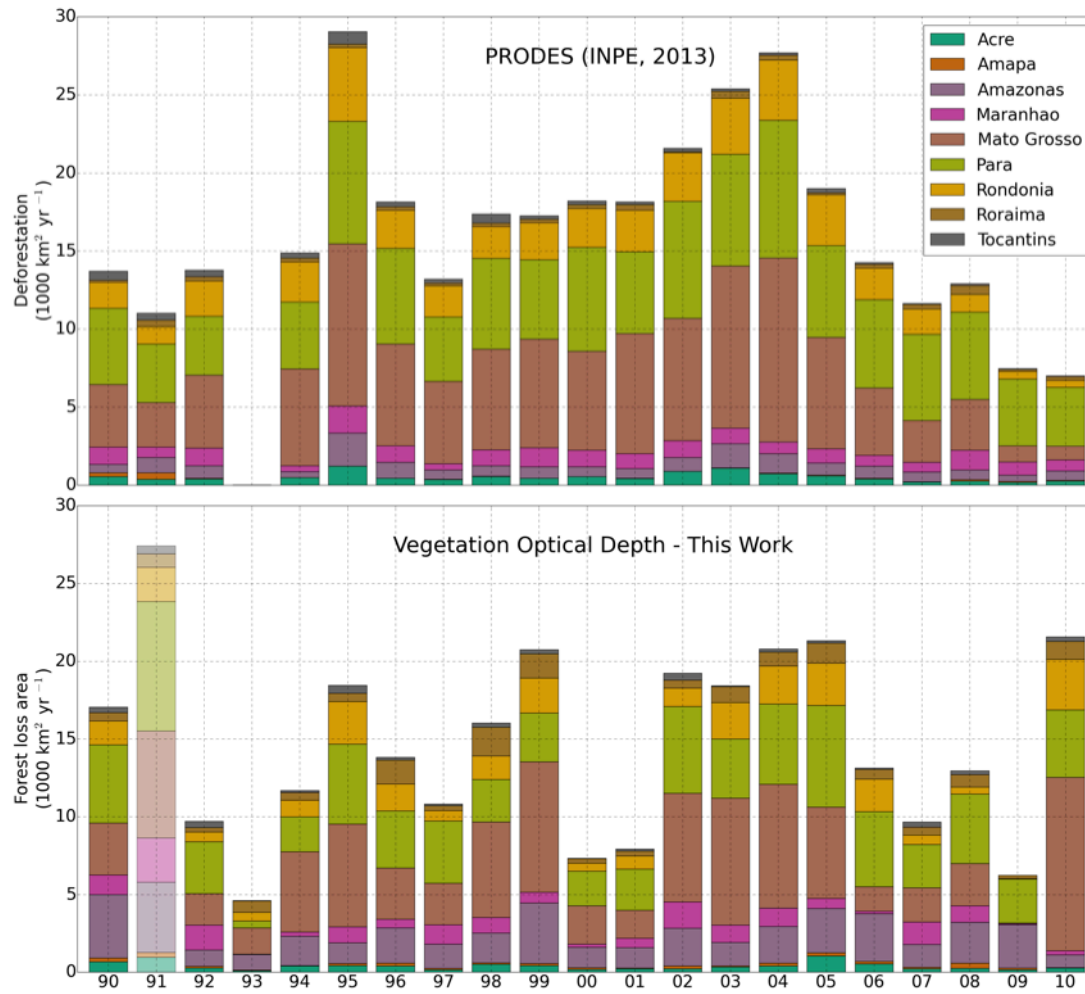
5



1

2 Figure 7. Country-level time series of annual totals of forest loss according to GFC (2001 -
 3 2010) and VOD (1990 - 2010). . VOD data is unreliable for 1991 as a result of the eruption of
 4 Mount Pinatubo.

5



1
 2 Figure 8. Time series of deforestation (PRODES) and forest loss area (VOD) for the Brazilian
 3 states in the Amazon (1990 – 2010). PRODES deforestation data is missing for 1993. VOD
 4 data is unreliable for 1991 as a result of the eruption of Mount Pinatubo.